

CHAPTER 3

RESULTS AND DISCUSSION

3.1. Synthesis of ferrous phosphate nanoparticles

The synthesis of ferrous phosphate nanoparticles were carried out without adding any oxidizing and reducing agents under various initial Fe and P molar ratios in order to clarify effects of the molar ratio on the reaction mechanism. When the molar ratio was 0.5 M corresponding to the stoichiometric ratio in the synthesis reaction, the nucleation progressed rapidly in an initial stage of the hydrolysis, resulting in formation of the ferrous phosphate nanoparticles having a smaller size. On the other hand, when the molar ratio of Fe precursor was more and less than 0.5 M, the particle size increased because the ferrous phosphate nanoparticles grew up slowly using surplus Fe (OH)₂ under hydrolytic conditions according to the Schikorr reaction. The major driving force for the formation of the ferrous phosphate nanoparticles is believed to be the reduced solubility of the Fe (III) ions. The synthesized ferrous phosphate nanoparticles were subjected to characterization to know the elemental content, morphological character, surface characteristics etc. The results obtained were as follows.

3.2. Characterization of nanoparticles

3.2.1. Elemental analysis by XRF spectroscopy

X-ray fluorescence spectroscopy results reveal the quantitative and qualitative elemental content of the ferrous phosphate nanoparticles. The X - rays emitted from the ionizing atom have energies, characteristic of the element involved and the intensity is proportional to the concentration of an element. The major elemental content as expected was found to be Fe and P, with some trace elements such as Mn, S and Ti. The variations in the Fe to P percentage were observed (Table

3.1.) for the different mode of synthesis and these changes are in relation with the molar ratio of the synthesis precursors. The Figure 3.1. indicates that the sample contains the elements Fe, P, S, Mn, Ca and Ti. Likewise the three different concentration syntheses were selected to cover elements in various parts of the periodic elements.

The major element Fe with contents of 72.70 % wt, 65.30 % wt and 54.65 % wt were found in the three different synthesis (A, B and C). The content of P was 25.92 % wt, 31.30 % wt and 42.25 % wt respectively in A, B and C synthesis. The minor elements S, Mn, Ca and Ti with content values of less than 1.0 % wt were found in all three synthesis.

The stoichiometric concentration of synthesis in this study has created much interest, since it showed the maximum Fe content resulting beneficial for the Fe bioavailability study.

Table 3.1 The elemental contents present in the ferrous phosphate nanoparticles examined by XRF spectroscopy.

SAMPLES	MAJOR ELEMENTS (%)		TRACE ELEMENTS (%)			
	Fe	P	S	Mn	Ca	Ti
A	72.70	25.92	0.67	0.59	0.11	-
B	65.30	31.30	2.81	0.23	0.10	0.18
C	54.65	42.25	0.62	0.64	0.25	0.32

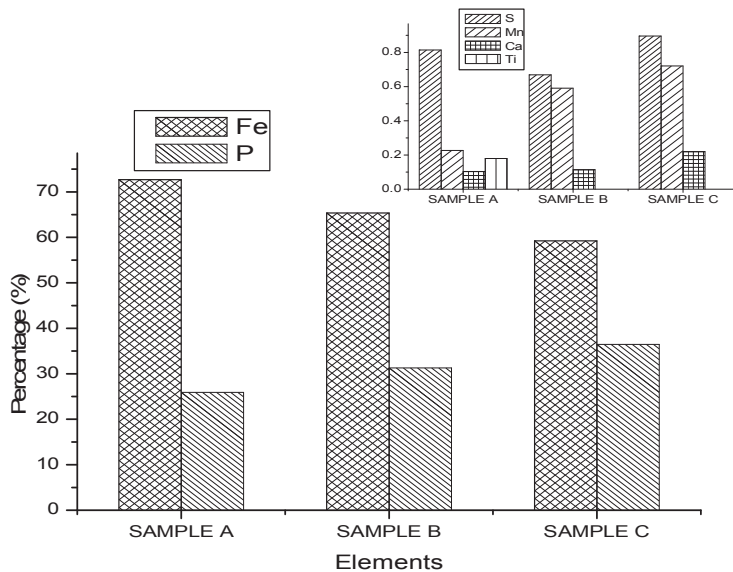


Figure 3.1 Histogram shows the level of elements present in the sample A of ferrous phosphate nanoparticles examined by XRF spectroscopy.

3.2.2. Fourier Transform Infra Red (FTIR) spectroscopic analysis

The infra red spectra of the synthesized particles were recorded to obtain the stretching vibrations of the functional groups present. The infra red spectrum of these particles after synthesis presented two regions. In the spectra, the bands centered at 3450 cm^{-1} and 1630 cm^{-1} are attributed respectively, to the O-H stretching and O-H-O bending of the water molecules. The peak around the 3450 cm^{-1} was found to be a broad one and the other corresponding peak at 1630 cm^{-1} was found to be a sharp stretching. From the O-H and H-O-H stretching shown in the Figure 3.2, it can be concluded that the water molecules are adsorbed with particles, synthesized through hydrolysis method.

The bands in the range of $1000 - 1200\text{ cm}^{-1}$ corresponds to the P-O stretching vibrations. The band that remained around the 562 cm^{-1} was attributed to the Fe-O stretching.

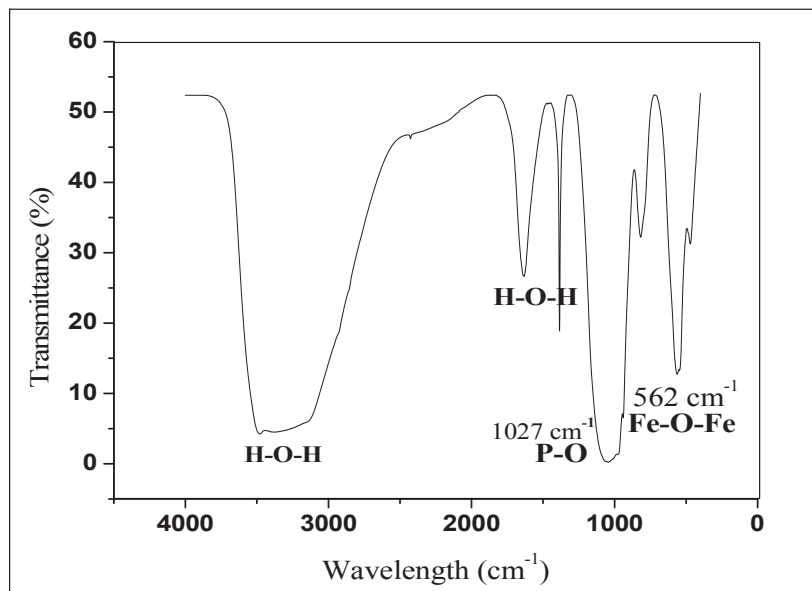
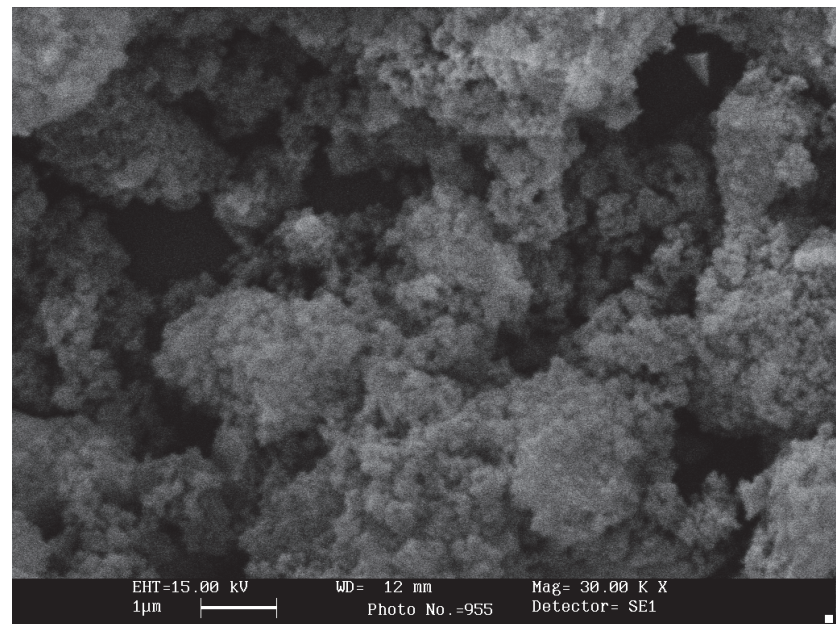


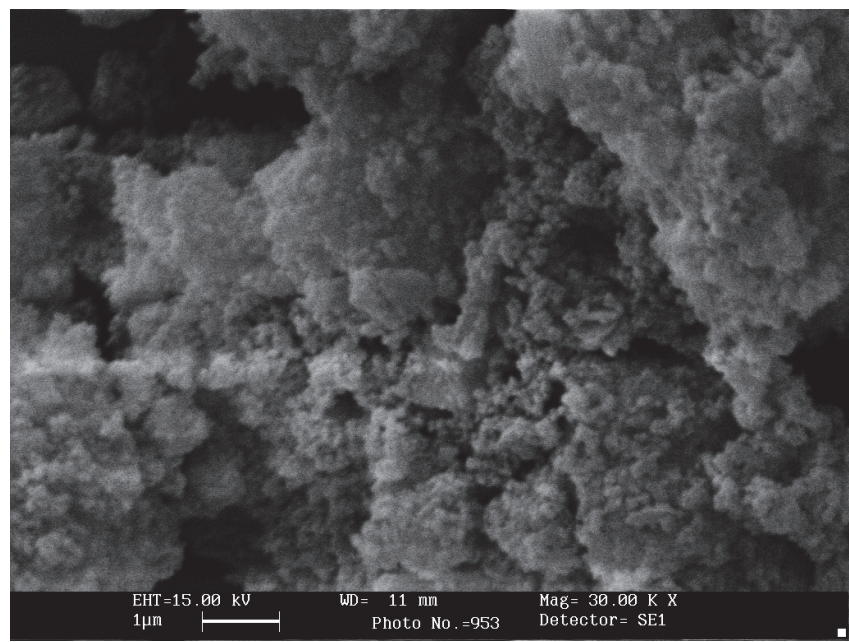
Figure 3.2 The peaks corresponding to the elements functional group analysed by FTIR spectroscopy

3.2.3. Scanning Electron Microscopy (SEM) studies

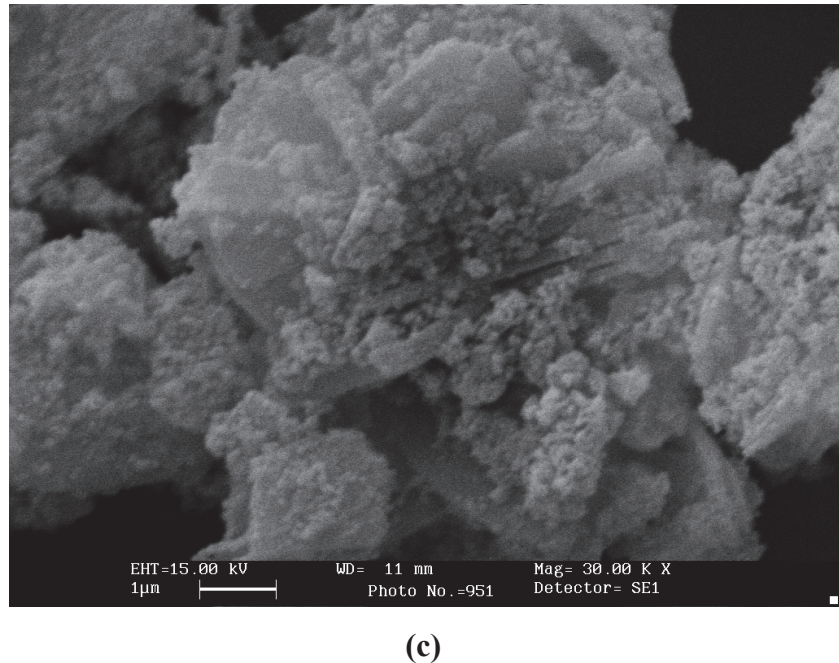
The structural features of the synthesised particles were examined using scanning electron microscopy. SEM is considered to be an important tool to analyze the formation of metal nanoparticles. The sample placed in the metallic stub coated with the gold sputtering was scanned in an area of $1\mu\text{m}$. The SEM micrograph (Figure 3.3. a, b & c), showed a sponge like structural arrangement due to the aggregation of the particles, taken immediately after the filtration process of synthesis in order to observe the bulk nature of the particles. The micrograph showed the spherical shaped structure in all the three synthesis modes, irrespective of the molar concentration of the precursor elements.



(a)



(b)



(c)

Figure 3.3 (a, b & c) The sponge like nature of the particles scanned at different areas of prepared sample by SEM analysis

3.2.4. Atomic Force Microscopy (AFM) studies

The individual particle morphology was well studied using the AFM image. To determine the topography of the ferrous phosphate particles, the sample was dispersed, coated in a glass substrate using the spin coater unit, dried and the surface was scanned in an area of 5.7 μm to 2.54 μm . The nanoparticles were found to be highly dispersed and are spherical in morphology. The two dimensional topography of the ferrous phosphate nanoparticles were shown in the Figures 3.4. to 3.6. Direct observation of the image revealed that the particles appear in spherical shape. The difference in the molar concentrations during the synthesis process does not alter the shape of the particles.

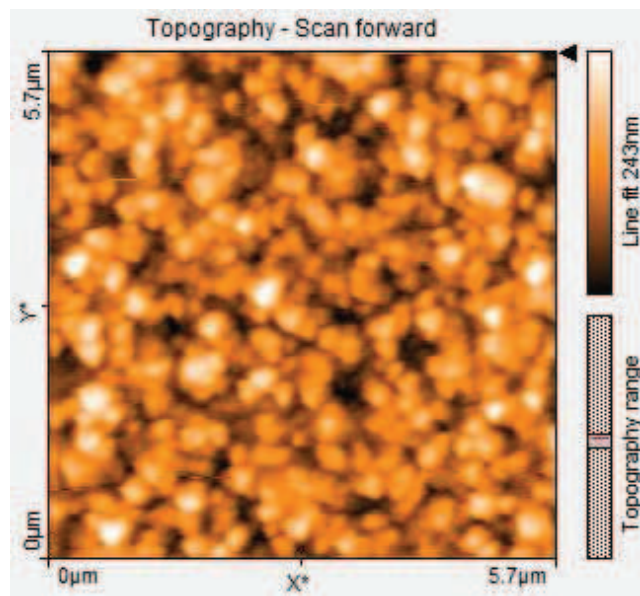


Figure 3.4 The spherical shaped particles analysed by AFM at 5.7 μm dimension

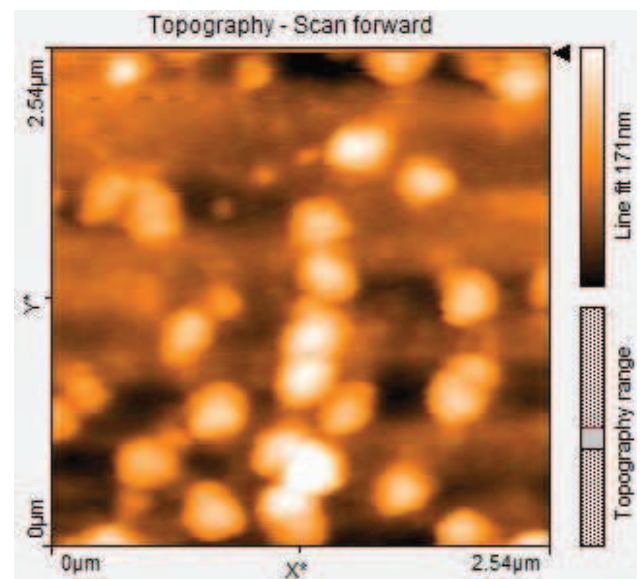


Figure 3.5 The spherical shaped particles analysed by AFM at 2.54 μm dimension

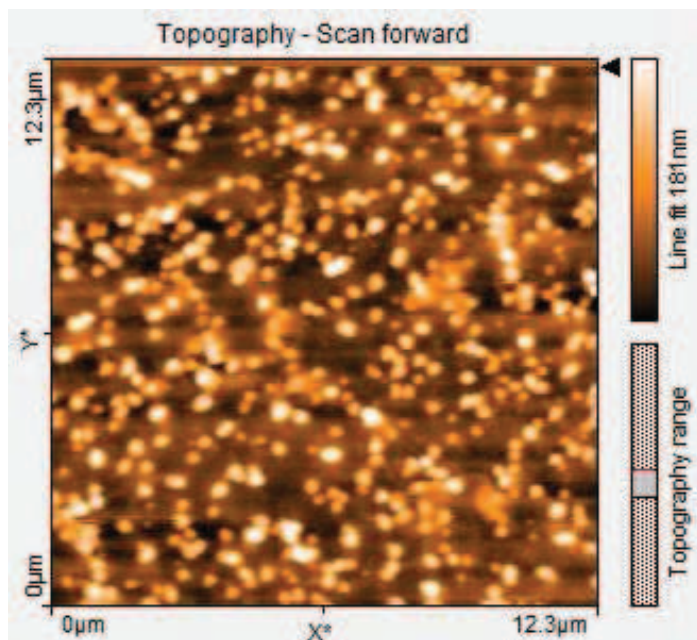


Figure 3.6 The spherical shaped particles analysed by AFM at 12.3 μm dimension

3.2.5. Particle Size Distribution analysis

The size distributions of the particles were observed using the centrifugal particle size analyser. Dramatic changes in the populations and sizes of the nanoparticles were observed when the concentrations of sodium phosphate and ferrous sulphate were systematically changed. Though the shape and morphology were found to be unique for all three synthesis concentrations, the difference in molar ratio was found to have influenced the size of the particles. The histogram of the sample A (Figure 3.7.) shows that the diameters of the particles were in the range of 70 – 110 nm. The size distribution study indicated that altering the concentration of the metal salt, tend to produce changes in the particle size of ferrous phosphate nanoparticles. The particle size distribution of the sample B and C were found to be in the range of 110 – 160 nm and 180 – 220 nm respectively (Figures 3.8. & 3.9.).

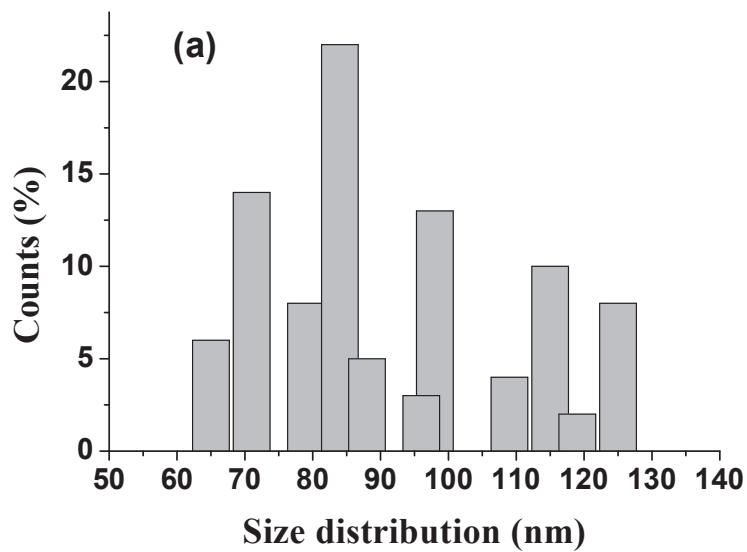


Figure 3.7 The particle size distribution of sample ‘A’ analysed using CPS particle size analyser

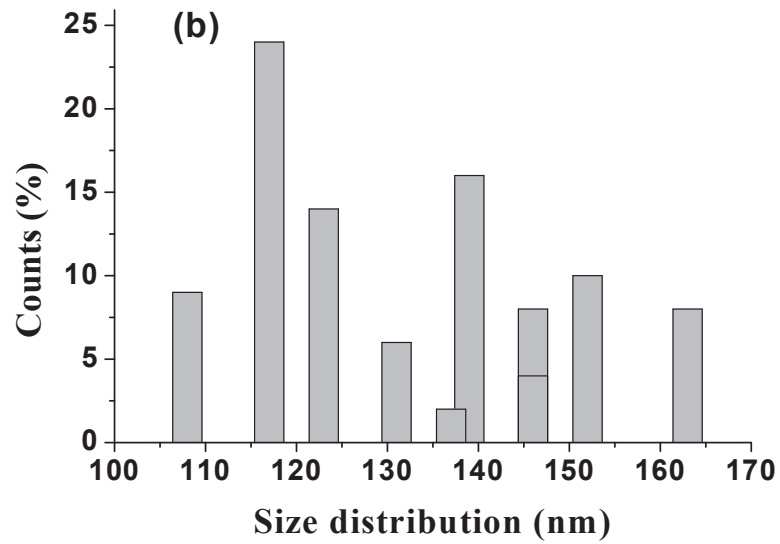


Figure 3.8 The particle size distribution of sample ‘B’ analysed using CPS particle size analyser

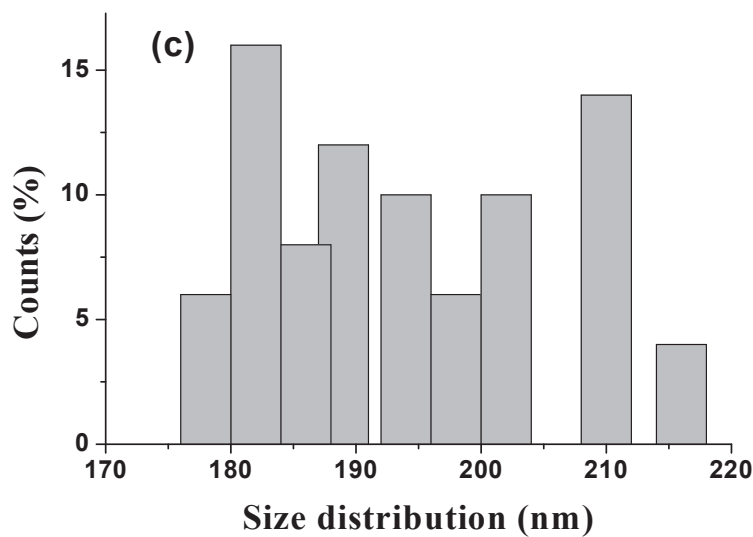


Figure 3.9 The particle size distribution of sample ‘C’ analysed using CPS particle size analyser

3.2.6. Specific Surface Area analysis (BET method)

Since, particle size of the compounds alone does not explain the differences in the bioavailability values, the samples were subjected for the analysis of specific surface area.

The surface area is a suitable parameter that can reflect the solubility of the iron powder. The surface area of the samples were analysed using the BET surface area analyser. As a general feature, the specific surface area of the particles obtained by different experiments synthesized ranged from 70 to 220 m²/g. The sample with low particle size revealed the maximum surface to volume ratio.

Here, we examine the influence of two parameters on the measurement of the specific surface area of nanostructured particles: the molar ratio of the precursors involved in the synthesis and the second parameter uncertainly linked to the diameter of the primary particles. The sample A with the low particle size diameter,

resulted in the higher mean specific surface area of $220\text{ m}^2/\text{g}$ than that of the other two sample synthesis.

The materials characterized for fairly strong specific surface area, depends on the particle size. As long as the particle size was smaller, the material depends to have larger specific surface area. As the particle size increased, the contribution of the surface area to the total decreased. The common factor of specific surface area underlies with the involvement of internal and external factors, for the particles with porous nature. The internal and external factors involved in the contribution of surface area are related to porosity and surface roughness. The relative importance of external and internal surface area is a function of the pore structure. Particles with an extensive network of fine pores are expected to have specific surface areas independent of particle size.

The ferrous phosphate particles with non porous nature, the specific surface area measurement were directly linked to the particle size diameter. Decrease in the particle size diameter, as in this case, was expected to result in the increase of particle specific surface area.

Table 3.2. Iron content and characteristic features of the ferrous phosphate nanoparticle

Sample	Fe Content (%)	Particle size range (nm)	Specific surface area (m^2/g)	Zeta Potential value (mV)
A	72.7	70-130	220	+ 6.8
B	65.4	110-160	104	+ 8.2
C	59.2	180-220	87	+ 13.8

3.2.7. Zeta potential analysis

Zeta potential is an important and useful indicator of the particle surface charge, which can be used to predict the stability of the synthesised particles. The zeta potential of ferrous phosphate nanoparticles were 6.8, 8.2 and 11.8 mV at pH 7.0 PBS (0.05 M). The particles possessed small positive charges at pH 7.0 indicating that a weak electrostatic repulsive force occurred between the particles. It was found to be beneficial in understanding the stability of the ferrous phosphate nanoparticles.

The results of the characterization of the synthesized nanoparticles (Table 3.2.) showed significant outcome with the sample ‘A’. The spherical shaped nanoparticles with low particle size and high specific surface area was found to be an advantageous reason to carry the sample A for the *in vitro* solubility study and *in vivo* analysis.

3.3. *In vitro* solubility analysis

The result of the solubility study indicates that the particles possess low solubility with water. This poor water solubility result resembles the report of EFSA, 2009 indicating that the ferrous phosphate powders are poorly soluble in water. To overcome these means, the ferrous phosphate nanoparticle powders were subjected to the dilute acid, to understand their acidic solubility.

The solubility and the dissolution of Fe ions in the HCl solution increased greatly, as the incubation time prolongs. The ferrozine indicator added to the 1.5 ml aliquot of each sample collected during each 15 minutes interval, produced light yellowish orange coloured solution as a result of interaction between dissolute Fe ions and pyridyl triazine of ferrozine, in the HCl solution. The OD values of the solution absorbance were found to be directly proportional to the intensity of the colour developed at 562 nm (Tables 3.3 & 3.4). The solubility rate was observed to be higher at pH 5 relatively to pH 2 of HCl solution. The Figure 3.10 shows the

solubility factor of prepared ferrous phosphate nanoparticles. A saturation level of absorbance was observed from the 60 min incubation time in pH 5 solution. The better dissolution in the higher pH was rated to be more advantageous, where it happens to have better absorption in the stomach.

This *in vitro* solubility testing method was rated to be with more accuracy since ferrozine has a better binding affinity to Fe (II) ions and their capability to detect even 0.2 mg/L.

Table 3.3 The *in vitro* solubility of sample ‘A’ at pH – 2 using ferrozine indicator

S.No.	pH of HCl	Time of aliquot taken (min)	Aliquot amount taken (ml)	Ferrozine added (ml)	Absorption OD value at 562 nm
1.	2.0	0	1.5	0.5	0
2.	2.0	15	1.5	0.5	0.09
3.	2.0	30	1.5	0.5	0.18
4.	2.0	45	1.5	0.5	0.28
5.	2.0	60	1.5	0.5	0.41
6.	2.0	75	1.5	0.5	0.49
7.	2.0	90	1.5	0.5	0.55
8.	2.0	105	1.5	0.5	0.62
9.	2.0	120	1.5	0.5	0.64

Table 3.4 The *in vitro* solubility of sample ‘A’ at pH – 5 using ferrozine indicator

S.No.	pH of HCl	Time of aliquot taken (min)	Aliquot amount taken (ml)	Ferrozine added (ml)	Absorption OD value at 562 nm
1.	5.0	0	1.5	0.5	0
2.	5.0	15	1.5	0.5	0.12
3.	5.0	30	1.5	0.5	0.26
4.	5.0	45	1.5	0.5	0.42
5.	5.0	60	1.5	0.5	0.57
6.	5.0	75	1.5	0.5	0.62
7.	5.0	90	1.5	0.5	0.65
8.	5.0	105	1.5	0.5	0.66
9.	5.0	120	1.5	0.5	0.67

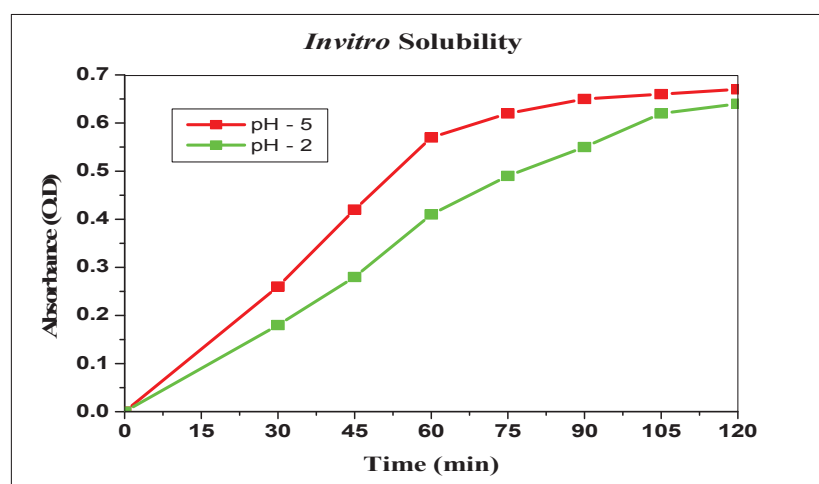


Figure 3.10 The *in vitro* solubility in HCL solution of sample A. The saturation levels of the Fe content dissolute were observed at the 60 min at pH 5

3.4. Formulation of biodegradable polymer encapsulated drug

To obtain the ideal formulation of chitosan microspheres and PLGA microspheres, preformulation studies were carried out using different variables. The variables were categorized as the independent variable and dependent variable. The drug to polymer concentration and the stirring speed applied for the preparation of microspheres were kept as the independent variables since it does not depends on any of the factor.

3.4.1. Formulation of Chitosan microspheres

Preformulation studies were carried out in order to establish compatibility between the polymer and drug. Microspheres were prepared by solvent emulsion technique using chitosan as a polymer due to its hydrophobicity and release controlling properties.

Effect of polymer concentration

Polymer concentrations of 0.5, 1.0, 2.0 % w/v were selected for the preliminary trials. The 1 % w/v concentration showed the optimum and maximum sphericity whereas 0.5% w/v showed flake formation and 2.0% w/v showed high viscosity. The microspheres containing higher amount of the polymer (1:3 drug to polymer ratio) exhibited smoother surfaces than those of other preparations (1:1 and 1:2 drug to polymer ratio). The drug to polymer ratio has greatly affected the characteristics of the microspheres. The results were shown in the Table 3.5.

Effect of stirrer speed

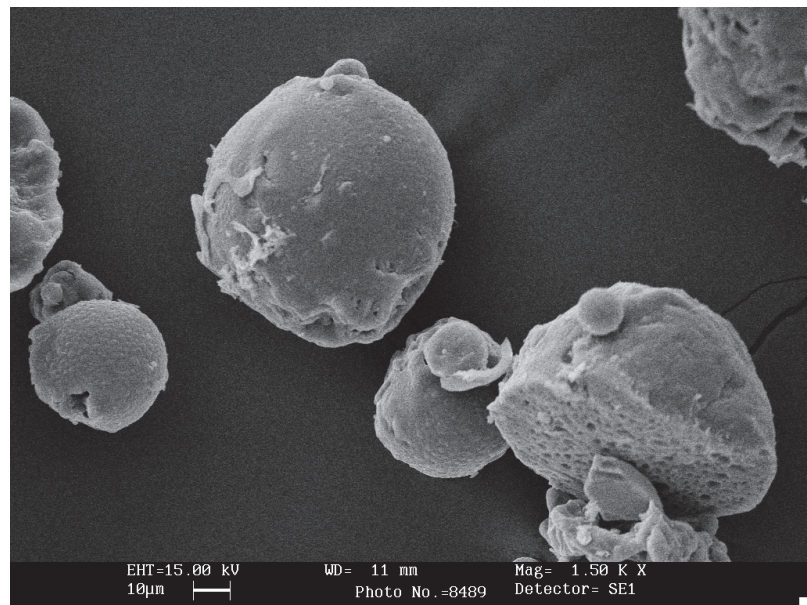
Various stirrer speeds of 1000, 1400 and 1800 rpm were used to find out the optimum speed necessary to obtain microspheres formation. From the results, it was found that 1800 rpm was the speed at which homogenous mixing of polymer in the dispersion medium took place and the microspheres were uniform sized and spherical in shape. The higher stirrer speed (1800 rpm) was difficult to work with

excessive splashing, it was found beneficial in the formation of microspheres and in the case of lower stirrer speeds (1000, 1400 rpm) it failed to convert the polymer into microspheres and showed clumping. The results were shown in Table 3.5.

Although, the shape of the microspheres in the low polymer concentrations showed the flake formation of particles in the low stirring speed, it tends to attain small spherical shaped particles at the higher stirring speed (Figure 3.11 a & b).

Table 3.5 The effect of polymer concentration and stirring speed on the shape of chitosan microspheres

Concentration of chitosan (w/v)	Stirring speed (rpm)	Uniformity
0.5 %	Minimum (1000 – 1400)	Small sized particles with flake formation
1.0 %	Minimum (1000 – 1400)	Regular and spherical shape
2.0 %	Minimum (1000 – 1400)	Large sized particles and showed high viscosity
0.5 %	Maximum (1800)	Small sized particles with spherical shape
1.0 %	Maximum (1800)	Regular and spherical shape
2.0 %	Maximum (1800)	Large sized particles and showed high viscosity

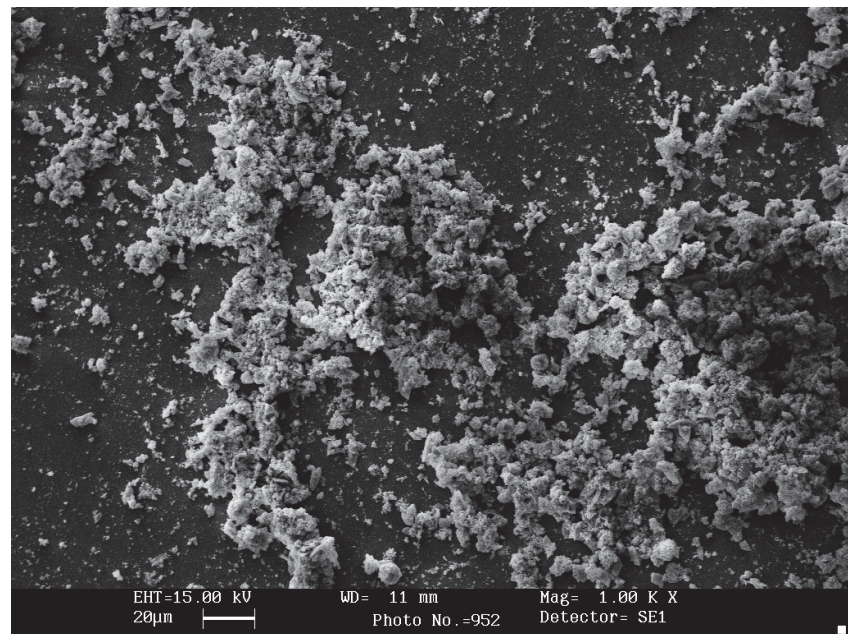


(a)

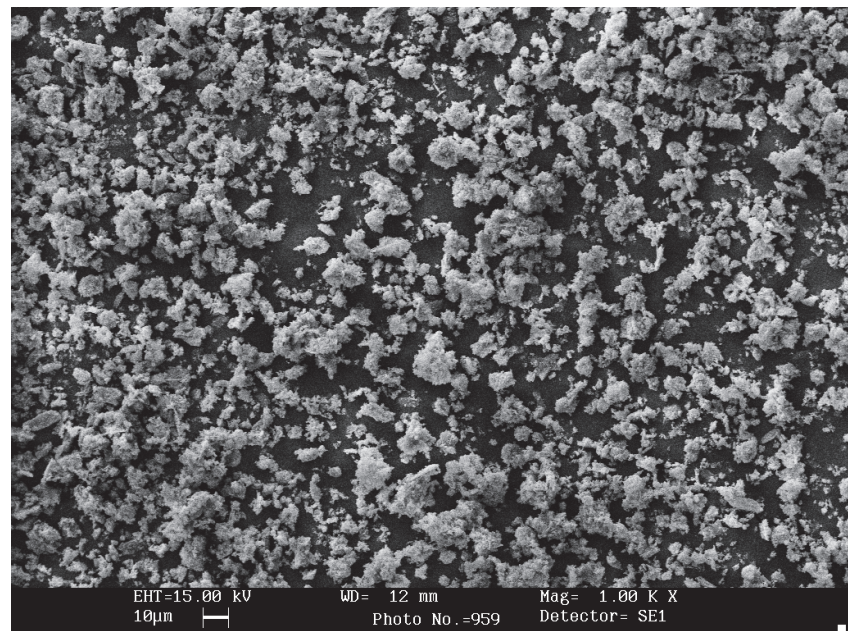


(b)

Figure 3.11 (a & b) The spherical shaped structure of the prepared chitosan microspheres analysed by SEM



(a)



(b)

Figure 3.12 (a & b) Irregular shape formation of the chitosan microspheres analysed by SEM

3.4.2. Formulation of PLGA microspheres

An attempt was made to formulate ferrous phosphate nanoparticles drug as microparticulate drug delivery system in order to localize drug at high absorption rate, reduced sensory effects, enhanced bioavailability thereby increased patient compliance. Microparticulate system was also formulated using PLGA carrier by solvent emulsion technique.

Effect of polymer concentration

In the preliminary trials of preformulation studies three concentrations of the polymer was employed (0.5, 1.0 and 2.0% w/v). The concentration 2.0% w/v of the PLGA polymer was tend to produce spherical shaped microspheres with smaller size, where, concentrations of 0.5% w/v and 1.0% w/v produced irregular shaped and flake formation respectively. As the earlier reports, the concentration of the drug to polymer ratio has a great influence on the characteristics of the microspheres.

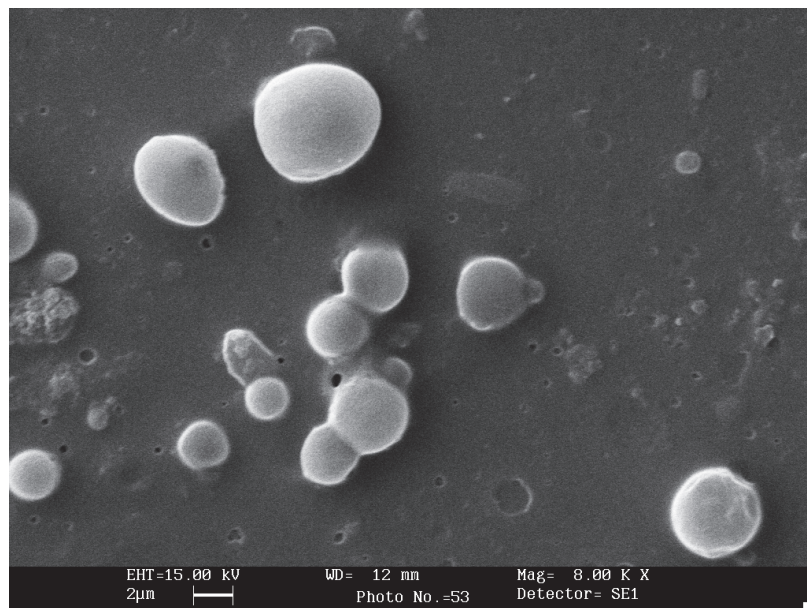
Effect of stirring speed

The preformulation studies were carried to find the effect of stirring speed on the microspheres formation. From the results, 800 and 1200 rpm shows lesser yield and highly irregular. The 1600 rpm showed highly uniform sized, spherical, higher yield and smooth surfaced microspheres, even though more splashing were observed.

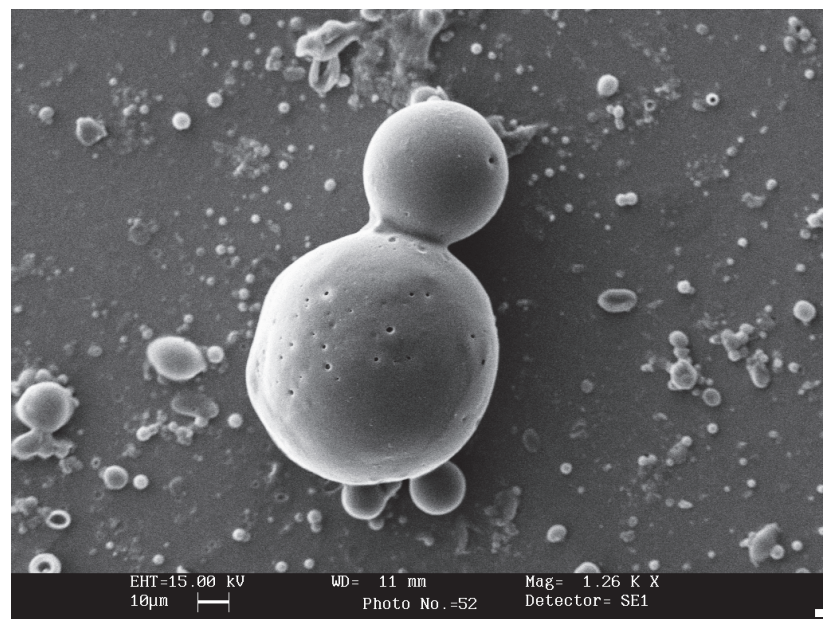
The results were shown in Table 3.6. The scanning electron microscopic (SEM) images of the various stirrer speeds were shown in Figure 3.12 a, b & c.

Table 3.6. The effect of polymer concentration and stirring speed on the shape of PLGA microspheres

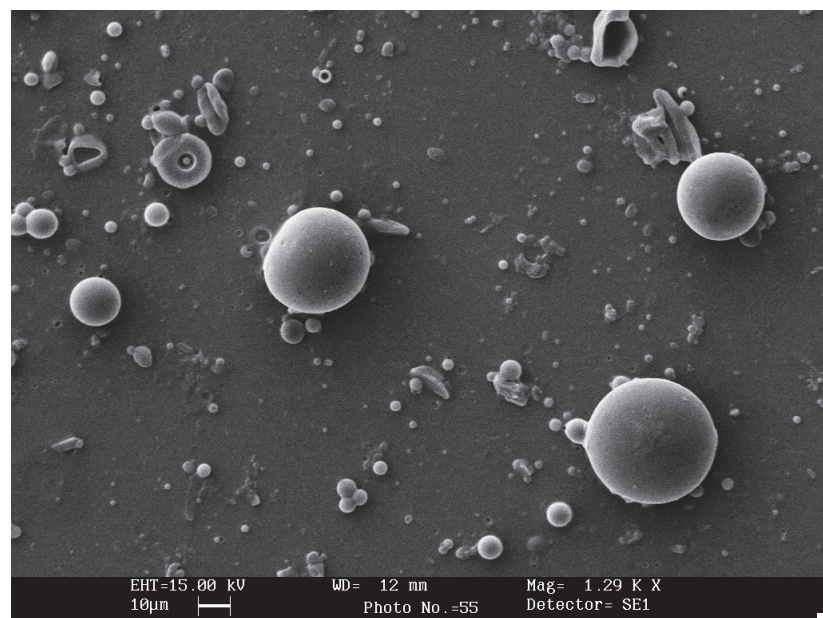
Concentration of chitosan (w/v)	Stirring speed (rpm)	Uniformity
0.5 %	Minimum (800 – 1200)	Small sized particles irregular shaped formation
1.0 %	Minimum (800 – 1200)	Regular and spherical shape
2.0 %	Minimum (800 – 1200)	Small sized particles and showed high viscosity
0.5 %	Maximum (1600)	Small sized particles with spherical shape
1.0 %	Maximum (1600)	Regular and spherical shape
2.0 %	Maximum (1600)	Small sized particles and showed high viscosity



(a)

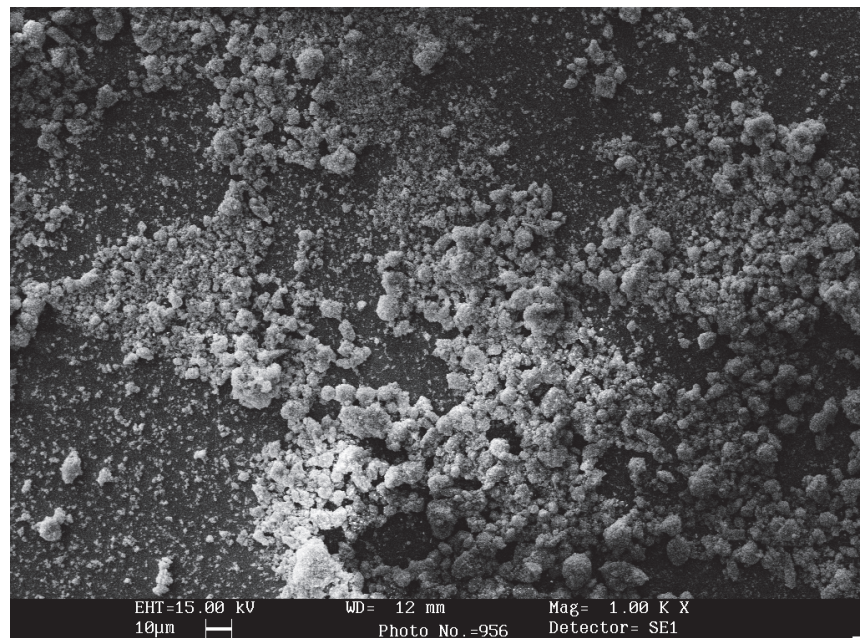


(b)

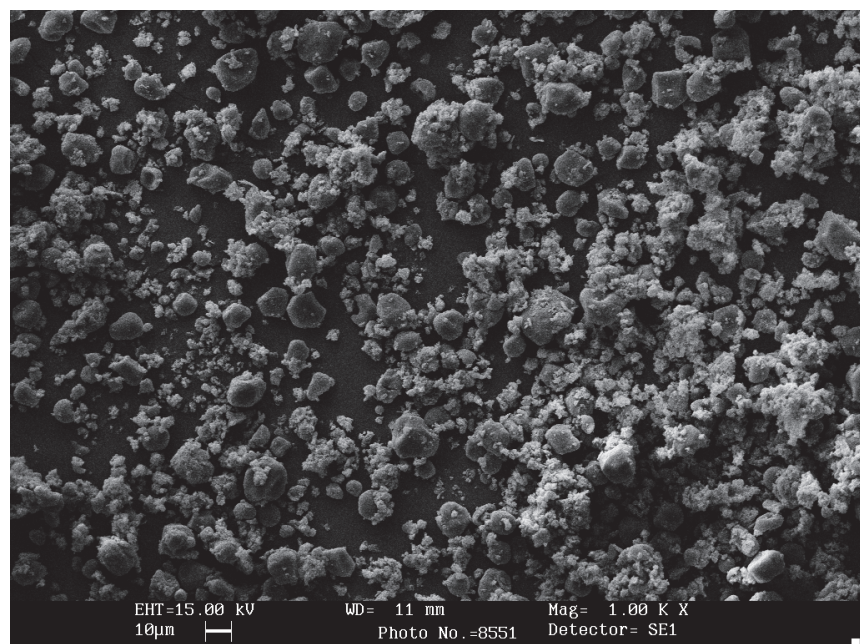


(c)

Figure 3.13 (a, b & c) The spherical shaped structure of the prepared PLGA microspheres analysed by SEM



(a)



(b)

Figure 3.14 (a & b) The irregular shape formation of the PLGA microspheres analysed by SEM

3.5. Characterization of the microspheres

The synthesized microspheres were subjected to the characterization for the particle size, percentage yield of the microspheres, drug entrapment efficiency and drug release profile using the invitro studies. The results of the characterization of the chitosan and PLGA microspheres were shown in the Tables 3.8 & 3.10. The optimal batch was found subjecting it to the Response Surface Methodology technique.

3.6. Response Surface Methodology for polymer encapsulation

The process of optimization by 3^2 factorial design needs that experimentation should be completed, so that the mathematical model can be generated. The number of experiments required for the studies depend upon number of independent variables selected. The experimental design was generated based on the general factorial design using Design Expert Software 8.0 (Stat-Ease, USA).

On the basis of the preliminary trials a full factorial design was employed to study the effect of independent variables (i.e. drug to polymer ratio and stirring speed) on the dependent variables (i.e. Particle size, drug entrapment efficiency and drug release), using the Design Expert 8.0 Software. The independent variables were varied at three different levels and taken for the response prediction (Tables 3.7 & 3.8). The responses of 9 batches (B1 to B9) were noted and it has revealed that all the dependent variables are greatly dependent upon the independent variables (Tables 3.9 & 3.10).

The polynomial equation was used to draw a conclusion of the magnitude of coefficients and the mathematical sign carriers. All the polynomial equations were found to be statistically significant ($p < 0.01$).

The responses obtained based on the full factorial design has depicted that all the dependent variable responses of both the polymer microspheres model (Chitosan

and PLGA) have same unique properties concerned. The effect of independent variables on the dependent variables of both the polymers, tend to produce uniform responses except in the terms of values.

Table 3.7 The three catagoric levels of independent variables chitosan microspheres

Independent variables	Independent variable levels		
	Low (-1)	Medium (0)	High (1)
Drug to Polymer ratio, w/v (X1)	1:0.5	1:1	1:2
Stirring speed, rpm (X2)	1000	1400	1800

Table 3.8 The three catagoric levels of independent variables for PLGA microspheres

Independent variables	Independent variable levels		
	Low (-1)	Medium (0)	High (1)
Drug to Polymer ratio, w/v (X1)	1:0.5	1:1	1:2
Stirring speed, rpm (X2)	800	1200	1600

Table 3.9 The response effect of independent variables on dependent variables of chitosan microspheres

Batch	Variable levels		Particle size (µm)	Drug Entrapment Efficiency (%)	Drug Release (min)
	X1	X2			
B1	-1	-1	21	66	350
B2	-1	0	18	70	340
B3	-1	1	14	72	325
B4	0	-1	30	62	415
B5	0	0	27	67	380
B6	0	1	24	65	355
B7	1	-1	36	59	480
B8	1	0	31	57	510
B9	1	1	29	60	530

Table 3.10 The response effect of independent variables on dependent variables of PLGA microspheres

Batch	Variable levels		Particle size (μm)	Drug Entrapment Efficiency (%)	Drug Release (min)
	X1	X2			
B1	-1	-1	5	76	290
B2	-1	0	4	78	285
B3	-1	1	2	85	270
B4	0	-1	10	68	370
B5	0	0	8	72	338
B6	0	1	7	76	329
B7	1	-1	12	59	458
B8	1	0	11	63	455
B9	1	1	9	66	480

3.6.1. Response effect on particle size

The results of the factorial equation showed that, the effect of drug to polymer ratio is significant than the stirring speed, on the particle size formation. The stirring speed had a negative effect on the particle size (i.e. as the stirring speed increased, the particle size decreased). The contour plot design of the software tends to produce a linear model effect.

Response on Chitosan microspheres

The particle size analysis of the chitosan microspheres loaded with ferrous phosphate nanoparticle drug was found to be in the range of 10 – 40 μm (Table 3.8). The factorial equation for the particle size showed a good correlation effect of 0.9979. The results indicate that the effect of drug to polymer ratio (X_1) is more significant than the stirring speed (X_2). The stirring speed produces a negative effect on the particle size. The polynomial equation derived on the effect of particle size using the intercepts and a mathematical sign was given below.

$$Y = 25.56 - 7.89X_1^1 + 1.44X_1^2 + 3.44X_2^1 - 0.22X_2^2 - 0.44X_1^1X_2^1 - 0.44X_1^2X_2^1 + 0.56X_1^1X_2^2 + 0.22X_1^2X_2^2$$

The Figure 3.15 shows the interaction terms of the drug to polymer ratio and the stirring speed and their effect on the particle size. The figure indicates that the drug to polymer ratio directly effect the particle size (i.e. the lower drug to polymer ratio results in lower particle size) but the effect of stirring speed was found to be in reverse.

The Figure 3.16 shows the 3 dimensional surface plot of the response effect, on the particle size of chitosan microspheres. It was found that lower drug to polymer ratio and higher stirring speed shows the optimal result.

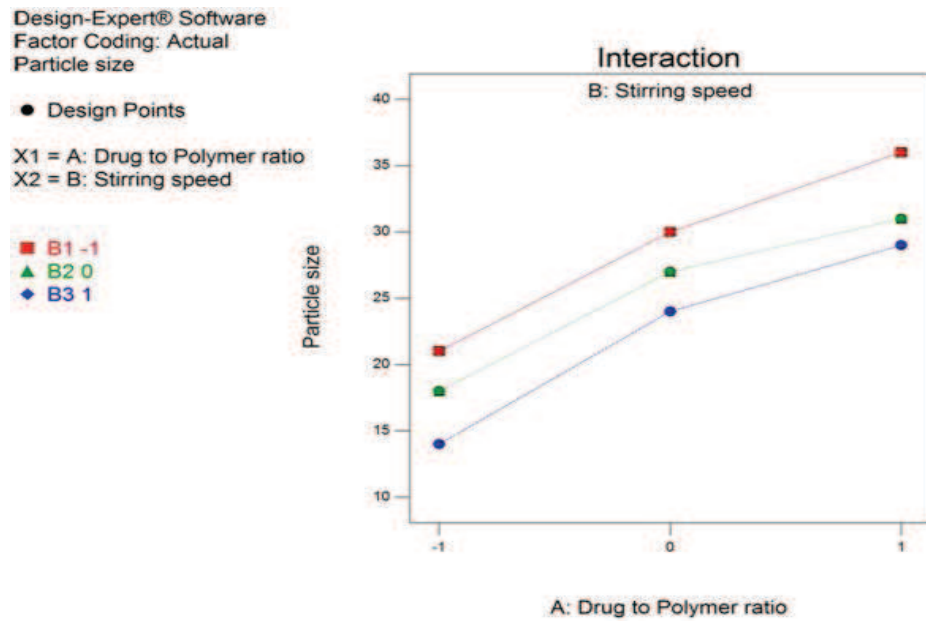


Figure 3.15 The contour interaction response effect on particle size of chitosan microspheres by RSM

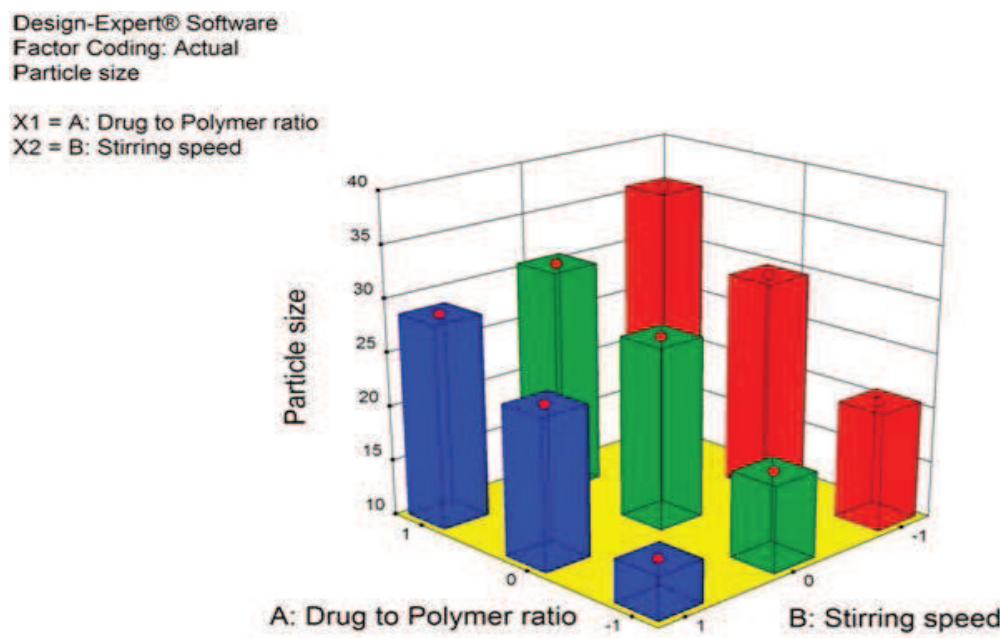


Figure 3.16 The 3 dimensional response effect on particle size of chitosan microspheres by RSM

Response on PLGA microspheres

The particle size analysis of the PLGA microspheres were found to be in the range of 0.9 – 10 μm . the particle size response showed a correlation coefficient of 0.907, which was rated to be a good effect. The narrow range of the particle size can be attributed to the effect of stirring time, stirring speed and the rate of solvent evaporation during the preparation of the microspheres.

The polynomial equation showing the intercepts and mathematical sign with respect to the response effect on particle size of PLGA microspheres was given below.

$$Y = 7.56 - 3.87X_1^1 + 0.78X_1^2 + 1.44X_2^1 + 0.11X_2^2 - 0.11X_1^1X_2^1 + 0.22X_1^2X_2^1 + 0.22X_1^1X_2^2 - 0.44X_1^2X_2^2$$

The Figure 3.17 relates the effect of particle size with the interaction terms of drug to polymer ratio and the stirring speed. Lesser the drug to polymer ratio results in lesser particle size. The Figure 3.18 shows the 3 dimensional surface plot of the response effect on particle size, pointing the surface plot lowered at the higher stirring speed and lower drug to polymer ratio.

As the stirring speed was increased, the size of the microdroplet of the emulsion was found to be decreasing, resulting in the formation of smaller microdroplets. The Figures 3.17 and 3.18 depict a linear trend of mean particle size in an ascending order with an increase in each variable. It concludes that, the drug to polymer ratio has comparatively greater influence on the response variables, than the stirring speed in particle size effect.

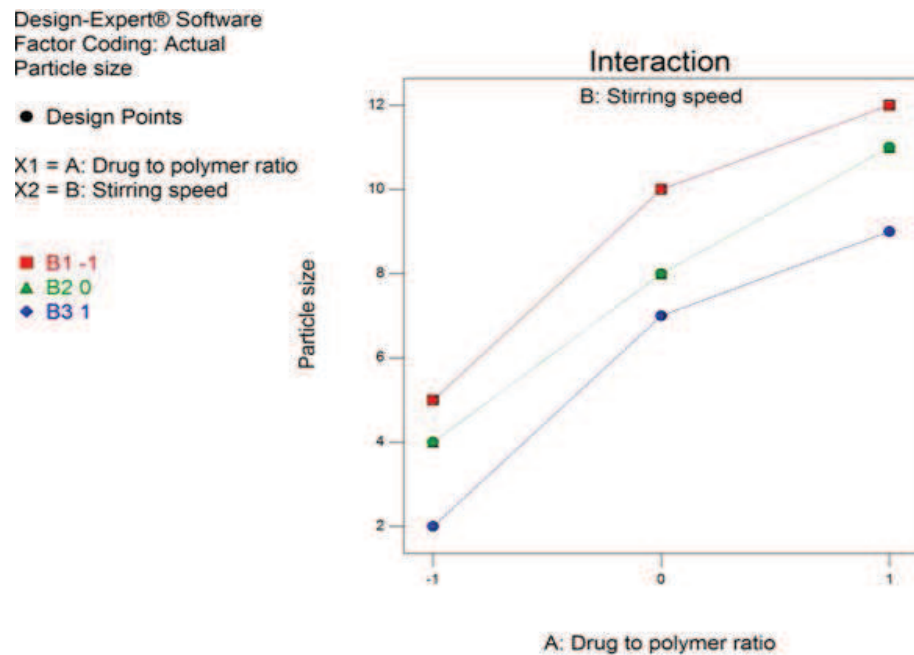


Figure 3.17 The contour interaction response effect on particle size of PLGA microspheres by RSM

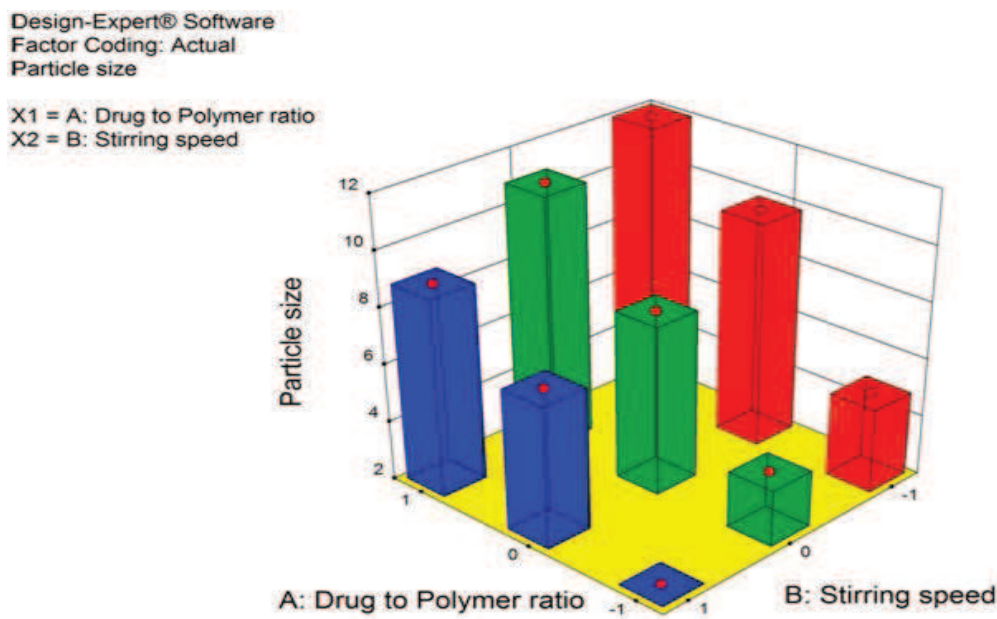


Figure 3.18 The 3 dimensional response effect on particle size of PLGA microspheres by RSM

3.6.2. Response effect on Drug entrapment efficiency

The results of the equation for the drug entrapment efficiency indicates that the effect of drug to polymer ratio was significant than the stirring speed, as in the case of particle size response.

Response on chitosan microspheres

The drug entrapment efficiency is a important variable for accessing the drug loading capacity of the microspheres. This parameter is dependent on the process of preparation, physiochemical properties of drug and formulation variables. The drug entrapment efficiency of the chitosan microspheres varied from 30 % to 65 % for most of the batches and it also showed a good correlation coefficient of 0.9970.

The result of the equation indicates the effect of the drug to polymer ratio (X_1) is more significant than stirring speed (X_2). The polynomial equation involving the intercept values along with the mathematical sign was given below.

$$Y = 64.22 + 5.11X_1^1 + 0.44X_1^2 - 1.89X_2^1 + 0.44X_2^2 - 1.44X_1^1X_2^1 - 0.78X_1^2X_2^1 + 0.22X_1^1X_2^2 + 1.89X_1^2X_2^2$$

The drug entrapment efficiency was found higher with the increase in drug to polymer ratio, which results in higher particle size. But the significant result was achieved only with the lower drug to polymer ratio which resulted in low particle size and also showing increased percentage of microspheres yield. Considering the way of single microsphere drug entrapment efficiency, the high polymer ratio ends with significance but the total yield of microspheres was found to be low. The Figure 3.19 shows the contour interaction terms of the drug entrapment in relation with the drug to polymer ratio and the stirring speed. The Figure 3.20 depicts the 3 dimensional surface plot to the response effect on the drug entrapment.

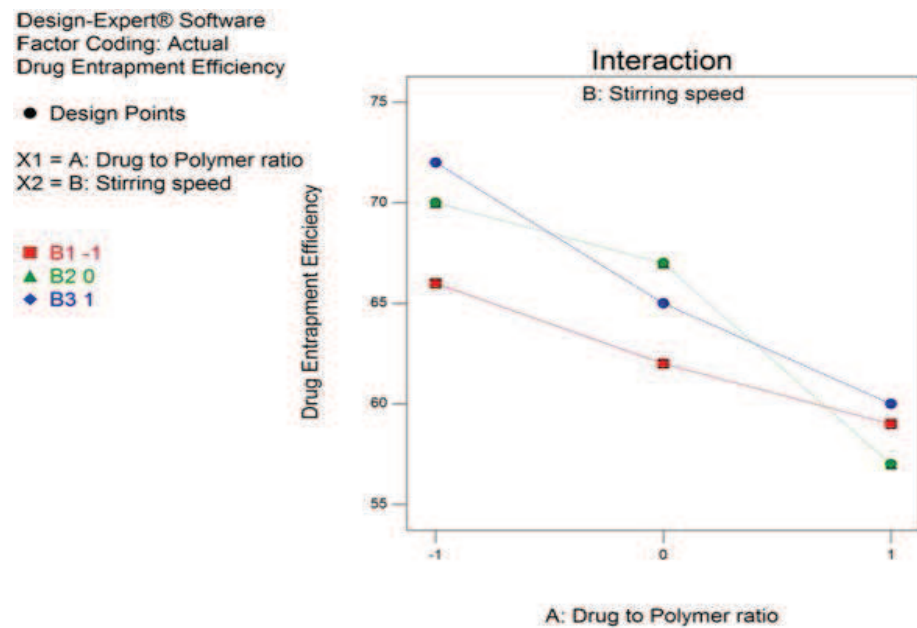


Figure 3.19 The contour interaction response effect on Drug Entrapment Efficiency of chitosan microspheres by RSM

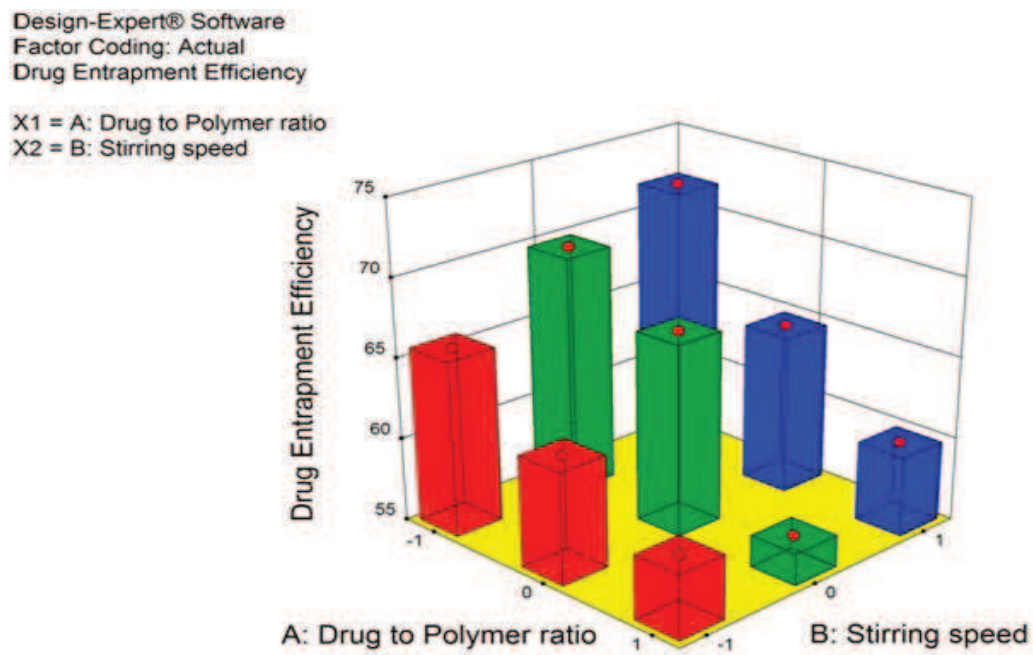


Figure 3.20 The 3 dimensional response effect on Drug Entrapment Efficiency of chitosan microspheres by RSM

Response effect on PLGA microspheres

The entrapment efficiency was found to be high in this case, showing 45 % to 80%. The polynomial equation with intercept values were found to be statistically significant ($p<0.01$) as determined using ANOVA as per the precision of Design expert software.

$$Y = 71.44 + 8.22X_1^1 + 0.56X_1^2 - 3.78X_2^1 - 0.44X_2^2 + 0.11X_1^1X_2^1 - 0.22X_1^2X_2^1 - 1.22X_1^1X_2^2 + 0.44X_1^2X_2^2$$

The Figure 3.21 shows the contour interaction groups of drug entrapment efficiency and the Figure 3.22 indicates the response effect of drug entrapment on PLGA microspheres, in 3 dimensional response surface plot.

The stirring speed had a positive effect on drug entrapment efficiency (i.e. as the stirring speed increased, the particle size decreased resulting in high yield of microspheres). As the drug to polymer ratio increase it produced large size particles thereby accommodating more drugs inside the microspheres, leading to decreased surface area. In this case, the diffusion of the drug will be very slow. But the significant optimal drug entrapment was calculated based on the total percentage yield of the microspheres, with low particle size and increased surface area. The entrapment efficiency varied in a non linear manner in ascending pattern with an increase in each variable but in the case of higher stirring speed, the contour lines tend to be linear. However the effect of drug to polymer ratio seems to be more pronounced as compared to stirring speed.

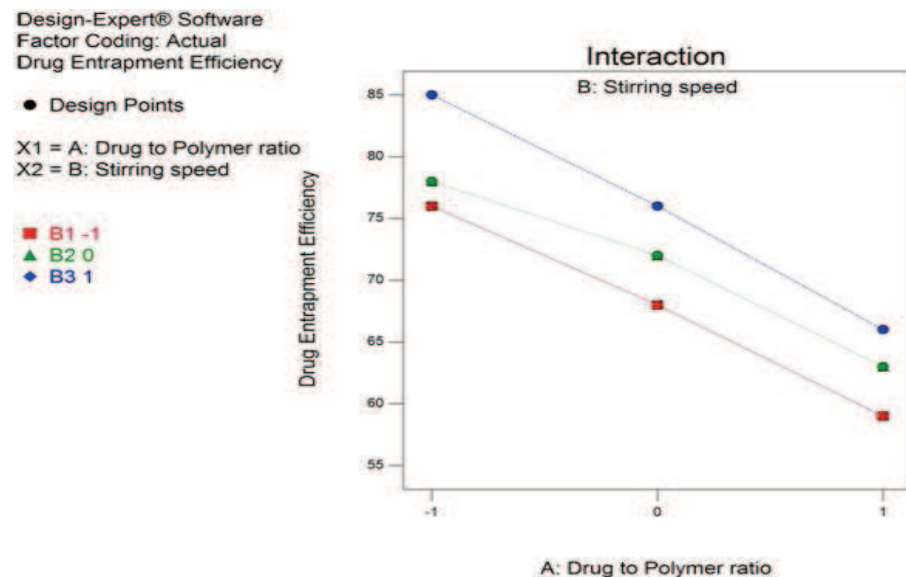


Figure 3.21 The contour interaction response effect on Drug Entrapment Efficiency of PLGA microspheres by RSM

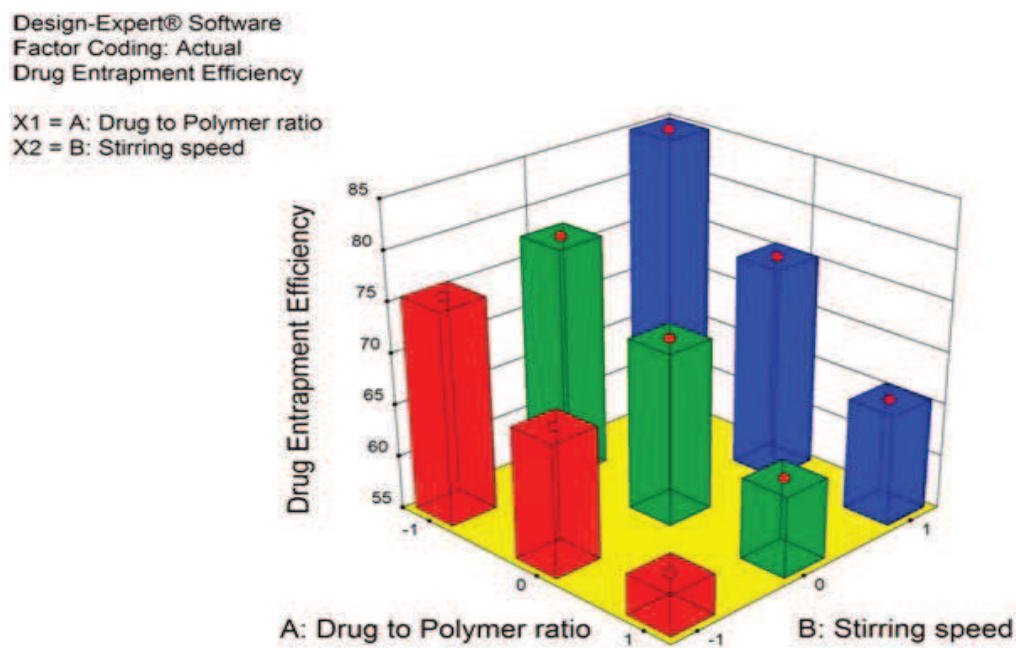


Figure 3.22 The 3 dimensional response effect on Drug Entrapment Efficiency of PLGA microspheres by RSM

3.6.3. Response effect on drug release

The release profile appears to be slow with negligible burst effect of the polymers. The low drug to polymer ratio exhibited higher initial burst in drug release, whereas the formulations showed little burst effect at higher drug to polymer ratio.

Response on chitosan microspheres

The release profiles of the formulations appear to be slow with negligible effect. The initial burst release of the drug was found in the lower level of drug to polymer ratio. The optimum values of the saturation level of ferrozine indicator colour formation, was observed from 320 min for the lower drug to polymer ratio, whereas the high levels of drug to polymer ratio showed the saturated drug release from 530 minutes. The batch B3 exhibited a high saturation level time.

The intercepts and mathematical sign involved in the polynomial equation of the response effect on drug release of chitosan microspheres was given below.

$$Y=409.44 - 71.11X_1^1 - 26.11X_1^2 + 5.56X_2^1 + 0.56X_2^2 + 6.11X_1^1X_2^1 + 26.11X_1^2X_2^1 + 1.11X_1^1X_2^2 - 3.89X_1^2X_2^2$$

The percentage *in vitro* drug release is highly dependent on the drug to polymer ratio and stirring speed. The polynomial equation indicating the mathematical sign, with the intercepts of X1 and X2 shows good correlation. The Figure 3.23 depicts the contour interaction terms of drug release in relation with the drug to polymer ratio and stirring speed. The low drug to polymer with high burst release varied with independent variables in a linear manner, where as the high drug to polymer ratio with slowly retarded release time, varied in a non linear way. The Figure 3.24 points the response effect on drug release, in a 3 dimensional response surface plot.

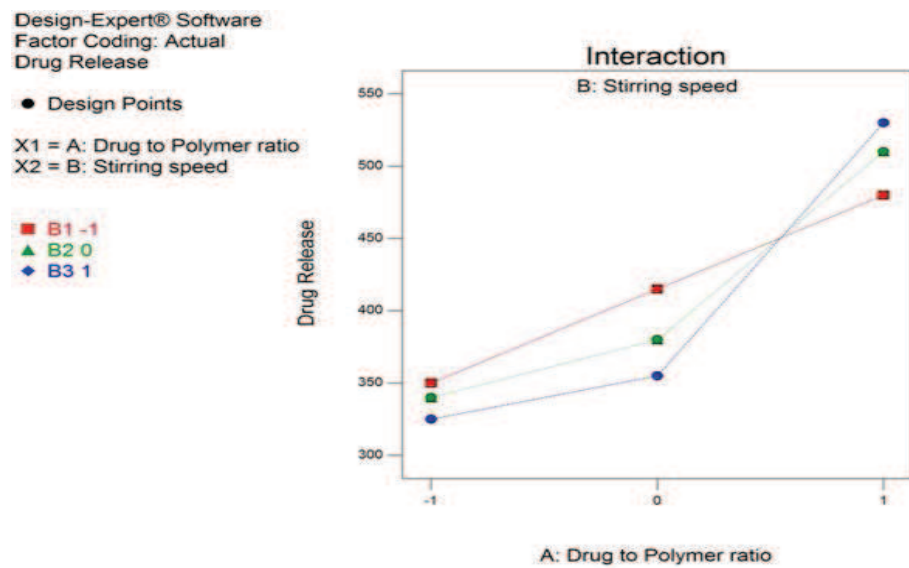


Figure 3.23 The contour interaction response effect on Drug Release of Chitosan microspheres by RSM

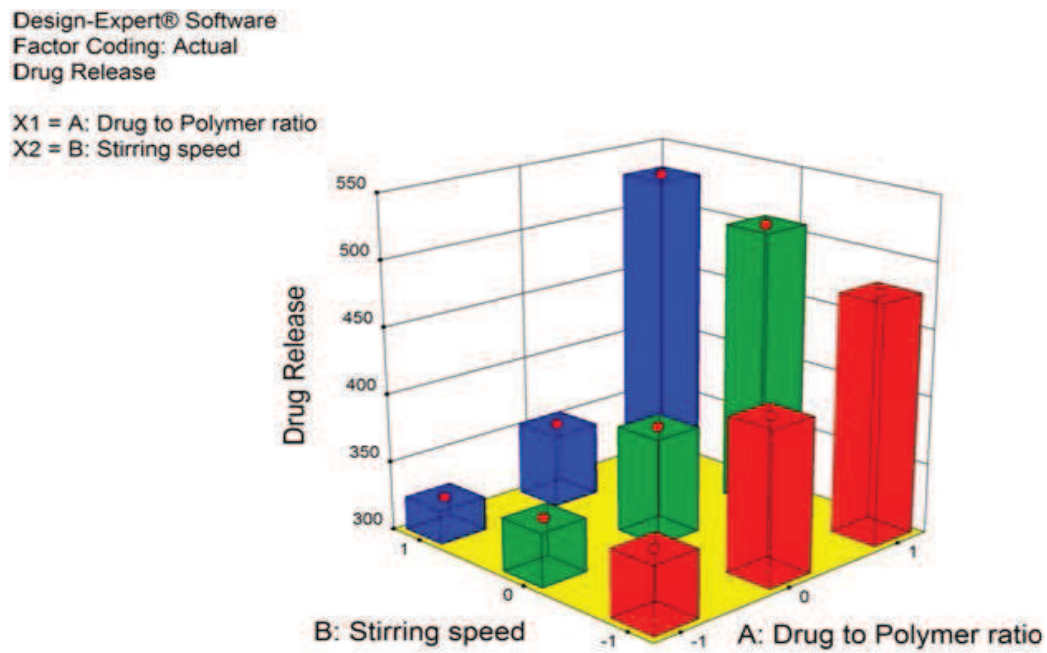


Figure 3.24 The 3 dimensional response effect on Drug Release of Chitosan microspheres by RSM

Response on PLGA microspheres

The drug release could be attributed to the dissolution of drug present, initially at the surface of the microspheres. However, the formulations showed little burst effect at higher drug to polymer ratio. The ferrozine indicator colour formation at saturation level enhanced markedly from 270 min, observed for a low level of drug to polymer ratio and to as high as 480 min observed at high level of drug to polymer ratio.

The polynomial equation with the intercept values and mathematical signs were indicated below.

$$Y = 363.89 - 8.22X_1^1 - 18.22X_1^2 + 8.78X_2^1 - 4.56X_2^2 - 0.44X_1^1X_2^1 + 15.56X_1^2X_2^1 + 7.89X_1^1X_2^2 - 3.11X_1^2X_2^2$$

Results depicted in the Figures 3.25 and 3.26 indicate the contour interaction terms and 3 dimensional response effect on drug release of PLGA microspheres. The effect of drug to polymer ratio (X_1) is more significant than the stirring speed (X_2). The stirring speed had a negative effect on the drug release, because as the stirring speed is increased, the particle size decreased thus leading to the initial burst of the microspheres. On the other hand, increase in the polymer matrix into the microspheres leads to an increased diffusional path and decreased drug release. Furthermore, smaller microspheres are formed at lower polymer concentration and has a larger surface area exposed to dissolution medium which is the reason for initial burst release of drug.

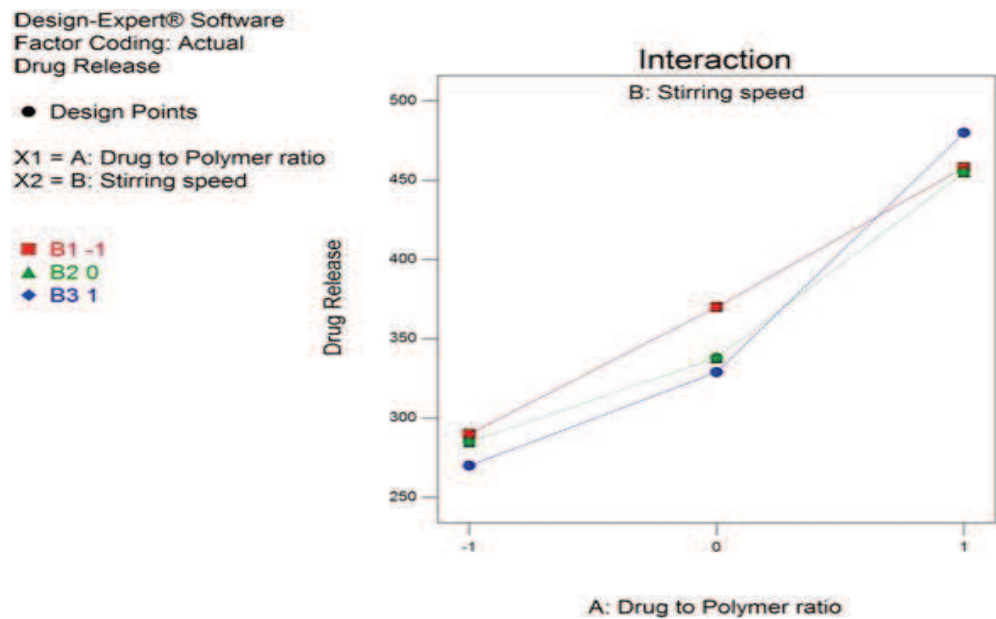


Figure 3.25 The contour interaction response effect on Drug Release of PLGA microspheres by RSM

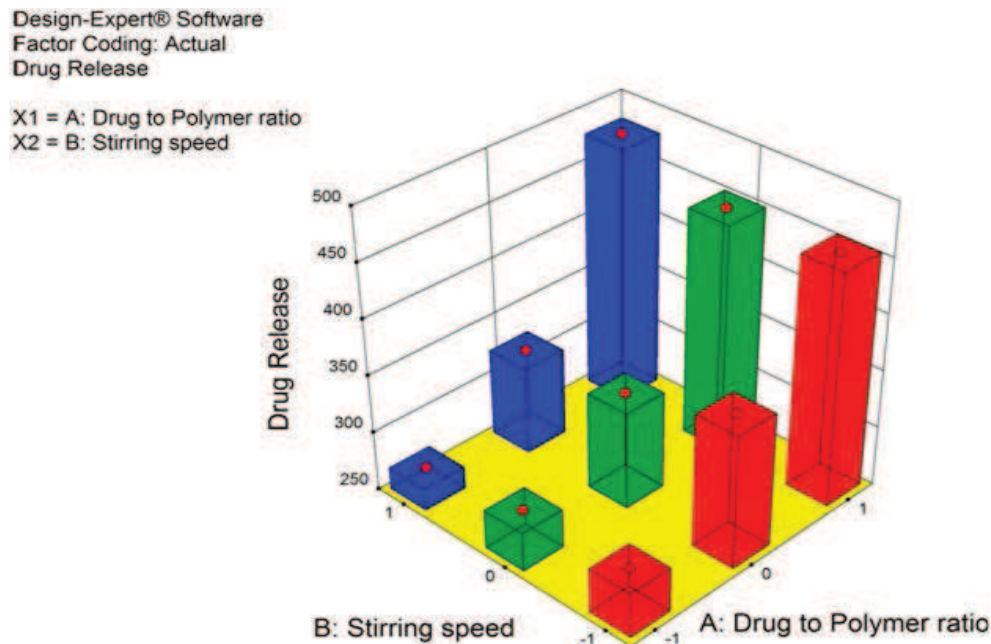


Figure 3.26 The 3 dimensional response effect on Drug Release of PLGA microspheres by RSM

3.6.4. Optimization of prepared microspheres

The numerical optimization was done using the design expert software based on the responses obtained from the 9 batches (B1 – B9). The desired goals were set for each responses and a solution was obtained to generate the optimal conditions. The graphical optimization was done by fixing the maximum and minimum limits for each response. The point prediction for the response was done by entering the desired operating conditions. Finally the confirmation of the optimal conditions was done by comparing the results predicted by the models. The optimum formulations of both the chitosan and PLGA microspheres were selected based on the criteria of attaining complete drug release with highest possible entrapment efficiency.

Optimization of chitosan microspheres

Upon the various response variables, the following maximizing criteria were adopted for the chitosan microspheres: Mean particle size <20 μm , entrapment efficiency > 60% and drug release saturation level obtained <330 minutes. To obtain the desired optimal conditions or batch, the goal of minimum particle size, maximum drug entrapment efficiency and with high initial burst drug release was fixed, with the design expert software. The solutions for 9 combinations of catagoric factor levels were predicted to find the optimum conditions. Finally, 7 possible solutions were obtained with the preference of the fixed goal (Tables 3.11 & 3.12).

The desirability bar graph (Figures 3.27 & 3.28) shows the optimum desirable level for obtaining the significant chitosan microspheres. The results of the 3^2 factorial design, revealed that the drug to polymer ratio and stirring speed are imperative to acquire good entrapment efficiency and enhanced drug release. The prepared chitosan microspheres of batch (B3) exhibited the mean particle size of 14 μm , entrapment efficiency of 72% and the maximum drug release at 325 min, was desired to be the optimal batch.

Table 3.11 The Analysis of variance (ANOVA) for the various responses of chitosan microspheres

	Particle size (μm)		Drug Entrapment Efficiency (%)		Drug Release (min)	
	F	P	F	P	F	P
X1	13.87	0.0025	18.60	0.0094	28.53	0.0043
X2	75.25	0.0001	1.90	0.2625	0.13	0.8827

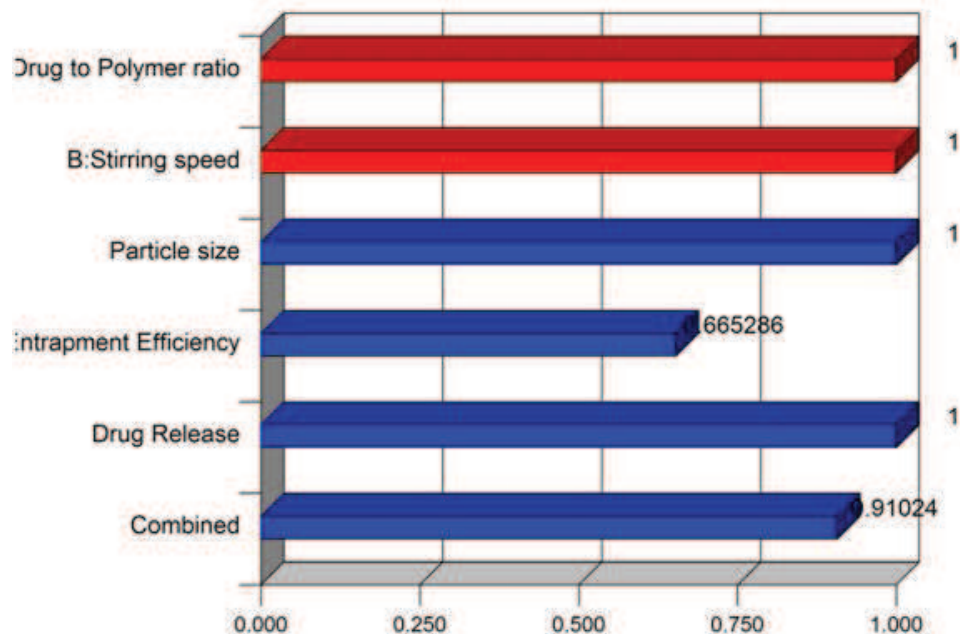


Figure 3.27 The bar graph of the desirability of optimal response of chitosan microspheres by RSM

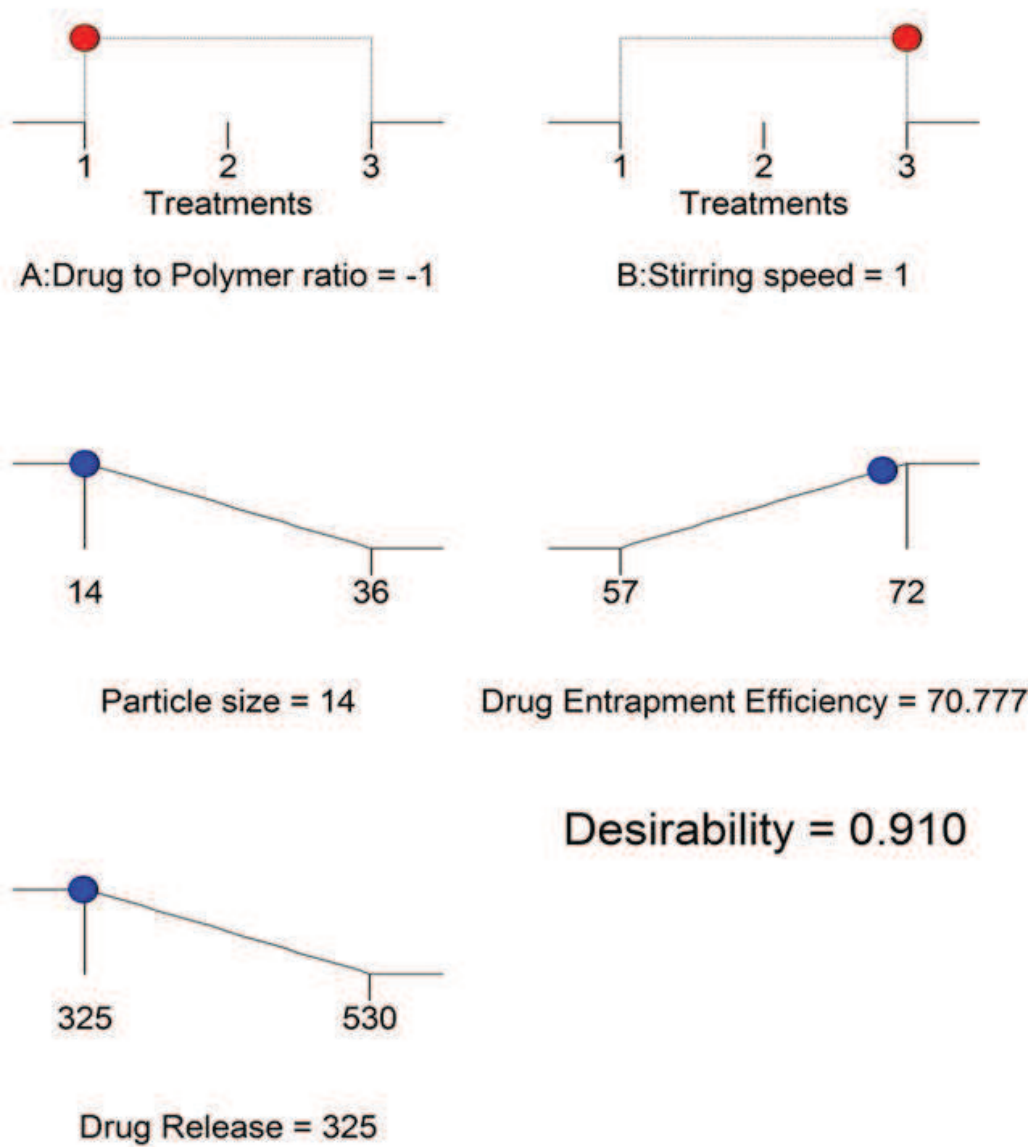


Figure 3.28 Graph ramp design showing the desirability of Chitosan microspheres by RSM

Table 3.12 The desired 7 batches of catagoric levels for optimal formulation of chitosan microspheres

S.No.	Drug to Polymer ratio (X1)	Stirring speed (X2)	Particle size (μm)	Drug Entrapment Efficiency (%)	Drug Release (min)	Desirability	w/o Intervals
1	-1	1	14	70.77	325	0.910	0.981
2	-1	0	18	69.77	340	0.804	0.866
3	-1	-1	21	67.44	350	0.701	0.755
4	0	1	24	66.11	355	0.617	0.664
5	0	0	27	65.11	380	0.506	0.506
6	0	-1	30	62.77	415	0.362	0.390
7	1	0	31	59.11	510	0.36	0.147

Optimization of PLGA microspheres

The following maximum criteria were adopted for the optimum PLGA microspheres: mean particle size <6 μm , drug entrapment efficiency >70% and the drug release saturation level obtained <290 minutes. For obtaining the ideal batch of PLGA microspheres, the optimization desirability goal was fixed as that of the previous one, with minimum particle size, maximum drug entrapment efficiency and enhanced drug release. The solutions of 9 combinations of catagoric factor levels were predicted for obtaining the optimal conditions. At last, 7 possible combinations were selected as per the preference of the goal fixed (Tables 3.13 & 3.14).

The desirability bar graph (Figures 3.29 & 3.30) depicts the optimum desirable level in obtaining the significant PLGA microspheres. The ideal batch for the optimized PLGA microspheres was selected to be B3, which exhibited mean particle size of 2 μm , entrapment efficiency of 85%, and maximum drug release at 270 min.

The formulated ideal batch of chitosan and PLGA microspheres were subjected to the *in vivo* analysis to know its effect on the haematological parameters.

Table 3.13 The Analysis of variance (ANOVA) for the various responses of PLGA microspheres

	Particle size (μm)		Drug Entrapment Efficiency (%)		Drug Release (min)	
	F	P	F	P	F	P
X1	16.33	0.0015	12.87	0.0032	101.87	0.0001
X2	61.00	0.0001	43.60	0.0003	101.87	0.0001

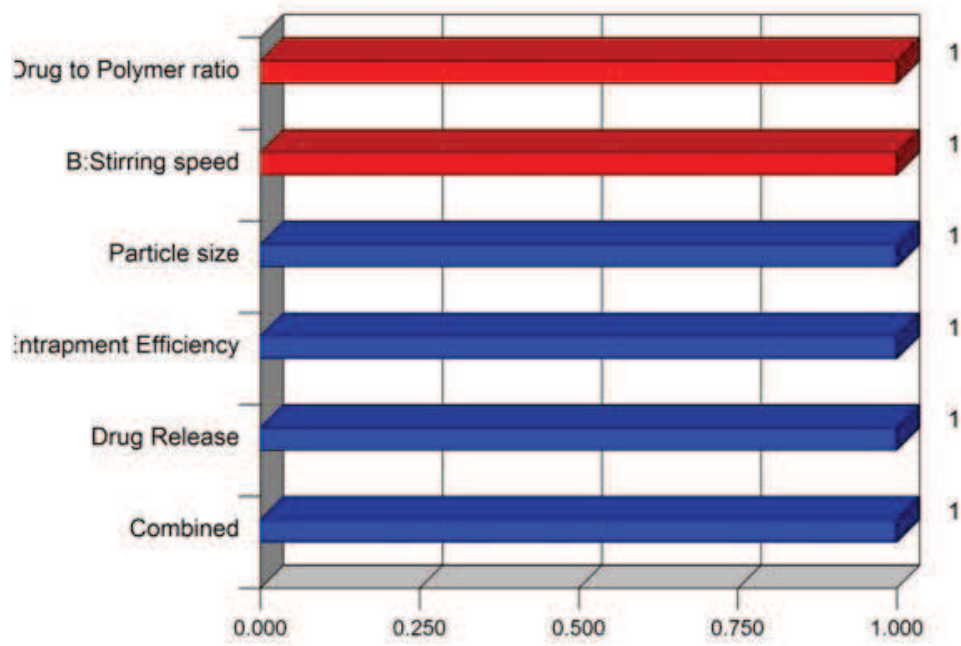


Figure 3.29 The bar graph of the desirability of optimal response of PLGA microspheres by RSM

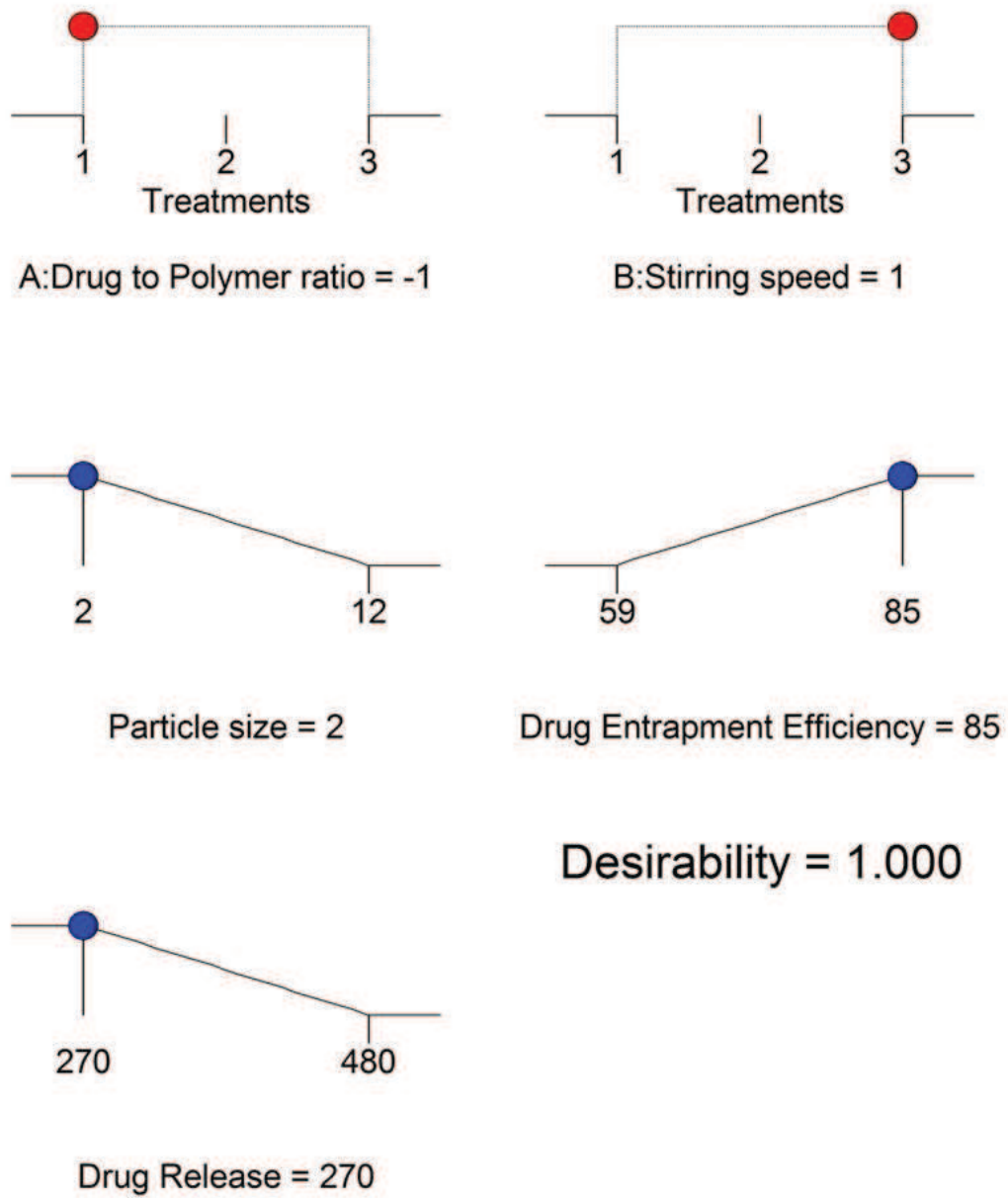


Figure 3.30 Graph ramp design showing the desirability of PLGA microspheres by RSM

Table 3.14 The desired 7 batches of catagoric levels for optimal formulation of PLGA microspheres

S.No.	Drug to Polymer ratio (X1)	Stirring speed (X2)	Particle size (μm)	Drug Entrapment Efficiency (%)	Drug Release (min)	Desirability	w/o Intervals
1	-1	1	2	85	270	1.000	1.000
2	-1	0	4	78	285	0.810	0.810
3	-1	-1	5	76	290	0.745	0.745
4	0	1	7	76	329	0.617	0.617
5	0	0	8	72	338	0.513	0.513
6	0	-1	10	68	370	0.331	0.331
7	1	0	11	63	455	0.122	0.122

Table 3.15 Summary of the 9 batch combination responses of chitosan microspheres

Response Name	Units	Batches	Analysis	Minimum	Maximum	Mean with S.D
Y1	Particle size	µm	9	Factorial	14	36
Y2	Drug Entrapment Efficiency	%	9	Factorial	57	72
Y3	Drug Release	min	9	Factorial	325	530

Table 3.16 Summary of the 9 batch combination responses of PLGA microspheres

Response Name	Units	Batches	Analysis	Minimum	Maximum	Mean with S.D
Y1	Particle size	µm	9	Factorial	2	12
Y2	Drug Entrapment Efficiency	%	9	Factorial	59	85
Y3	Drug Release	min	9	Factorial	270	480

3.7. *In vivo* analysis

The pharmacological effect of the ferrous phosphate nanoparticles has not previously studied extensively. Before screening for biological activity, the acute toxicity studies were carried out for the synthesized particles.

3.7.1. Acute toxicity studies

In toxicity studies the drug administered orally to rats upto the highest dose 30 mg/kg body wt. it does not produce any significant change in autonomic and behavioural responses during observation upto 8 hrs. The body weights were recorded on day 8 and 15. There were no gross necropsy findings during the study (Table 3.15.). Also animals did not exhibit any toxic signs like restless, respiratory distress, convulsions, coma etc.

3.7.2. Animal Experimentation

The Tables 3.16 and 3.17 shows the effect of ferrous phosphate nanoparticle drug on anaemia induced by phenylhydrazine hydrochloride. The reduction of PCV values by more than 50% of the baseline values in all rats at day 3, after phenyl hydrazine administration is an indication of anaemia. After anaemia has been induced in rats, daily oral treatment with the formulated drugs significantly increased the haematological parameters over the control. The effect of the formulation drugs on haematological parameters showed that there was significant differences ($p<0.05$) in the treated rats.

Remarkable antianemic activity was obtained with PCV of 50 – 58%, RBC count of $9 - 12 \times 10^6 / \mu\text{l}$ and Hb value of 17 – 20 g/dl after treatment with the ferrous phosphate nanoparticle drug direct uptake on day 9, compared with 26 % of PCV, $4 - 7 \times 10^6 / \mu\text{l}$ of RBC and 11 – 13 g/dl of Hb value in the rats treated with phenylhydrazine hydrochloride treated animals at day 3. Subsequent level of the haematological parameters was observed at the day 18, even after the two maintanence dose of phenylhydrazine at day 6 and 12.

The parameters observed for the polymer encapsulated drug treated animals, showed that the drug activity was slowed down with a PCV of 35 – 38%, RBC count of $7 - 9 \times 10^6 / \mu\text{l}$ and Hb value of 13 – 15 g/dl at the day 9 for the chitosan microspheres and PCV of 37 – 41 %, RBC count of $8 - 11 \times 10^6 / \mu\text{l}$ and Hb value of 16 – 18 g/dl for the PLGA encapsulated drug. This activity may be due to the cause of slow release of the drug from the polymers, but these factors are found to be advantageous in means of avoiding sensory effects. The observations of the polymers drug treated animals revealed the values above to the normal level of PCV, RBC and Hb in normal rats (40 – 47%, $7 - 9 \times 10^6 / \mu\text{l}$ and 13 -17 g/dl respectively) at the day 18. The biochemical estimation for the ferritin protein level indicated a high level during the day 18 for the nanoparticle direct uptake, Chitosan microspheres and PLGA microspheres treated animals (4-6 mg/dl, 3-4 mg/dl and 3-5 mg/dl) comparing to the normal rats with 2-4 mg/dl.

The significant effect of the orally treated drugs at various doses on the RBC and indices relating to it (PCV, Hb and ferritin level) throughout the experimental period is an indication that there was no destruction of matured RBC's and no change in the rate of production of RBCs (erythropoiesis). It further shows that the drugs administered have the potential to deliver the Fe compounds for the process of erythropoiesis which signifies to the increase in the haematological parameters. The significant effect on the RBC and Hb also implies that there was an increase in the oxygen-carrying capacity of the blood and amount of oxygen delivered to the tissues following the ferrous phosphate nanoparticle drug administration, since RBC and Hb are very important in transferring respiratory gases. Furthermore the final increase in the ferritin protein level depicts that the haematological parameters also results in the storage of iron binding proteins.

Table 3.17 The Body weights, body weight changes and preterminal deaths of acute toxicity studies

Dose mg/kg b.wt.	Rat	Sex	Gross necropsy findings	Body weight (g)				No. of dead / No. tested
				Weight initial	Weight 8 th day	Weight change upto 8 th day	Weight 15 th day	
1	Female	No abnormalities detected	152	180	28	192	40	
2	Female	No abnormalities detected	146	164	18	173	27	
3	Female	No abnormalities detected	159	185	26	196	37	
30	4	Female	No abnormalities detected	138	140	02	150	12
	5	Female	No abnormalities detected	163	196	33	201	38
	6	Female	No abnormalities detected	162	195	33	205	43

Table 3.18 Haematological evaluation (PCV & RBC values) of ferrous phosphate nanoparticle drug against phenylhydrazine induced anaemia

Treatment	PCV (%)				RBC ($\times 10^6$ μ l)			
	Day 0	Day 3	Day 9	Day 18	Day 0	Day 3	Day 9	Day 18
Control	44±3.03	43.8±2.71	44.6±1.21	44.3±1.50	6.51±0.33	6.85±2.88 ^a	6.95±0.36	7.18±0.31
Control induced	43.5±2.42	26.3±2.58 ^a	26.5±1.87 ^a	31.0±1.41 ^b	6.45±0.24	4.81±0.14 ^a	5.01±0.19 ^b	5.36±0.17
Ferrous phosphate drug	42.8±2.78	26.5±2.07 ^a	52.3±2.58	57±1.78	6.51±0.26	4.98±0.30 ^a	8.76±0.39	9.48±0.40
Chitosan microspheres	42.2±2.16	25.8±2.56	38.4±1.67	49.8±1.52 ^b	6.42±0.36	4.32±0.57	6.28±0.86	7.96±0.44
PLGA microspheres	43.2±2.36	26.3±2.76 ^a	41.4±1.84	53.1±1.42	6.33±0.40	4.56±0.23	7.14±0.18 ^b	8.39±0.53
Commercial drug	42.6±2.16	25.1±2.63 ^a	41.1±1.72	47.3±1.96	6.58±0.29	4.91±0.19 ^a	6.66±0.34	7.73±0.32

Mean values are expressed in terms of \pm SD.

a & b - indicates the significant variations in each homogenous subsets at $p<0.05$ level (5%) by Tukeys HSD test.

Table 3.19 Haematological evaluation (Haemoglobin & ferritin values) of ferrous phosphate nanoparticle drug against phenylhydrazine induced anaemia

Treatment	Haemoglobin (g/dl)				Ferritin level (mg/dl)			
	Day 0	Day 3	Day 9	Day 18	Day 0	Day 3	Day 9	Day 18
Control	14.31±0.40	14.45±0.42	14.5±0.52	14.46±0.51	4.28±0.40	4.25±0.30	4.36±0.43	4.33±0.43
Control induced	14.41±0.49	12.96±0.61 ^a	13.48±0.29	14.15±0.30	4.48±0.51	3.7±0.40	3.81±0.29	3.38±0.36 ^a
Ferrous phosphate drug	15.20±0.35	12.73±0.51 ^a	18.1±0.37	18.9±0.49	3.95±0.39	3.15±0.31 ^a	4.48±0.44	5.66±0.35
Chitosan microspheres	14.68±0.54	12.76±0.76	16.37±0.61 ^a	16.97±0.57	4.13±0.27	3.26±0.41	3.64±0.57	4.42±0.68
PLGA microspheres	14.34±0.24	12.42±0.64	17.31±0.72	17.91±0.81	4.42±0.15	3.41±0.53	3.91±0.61 ^a	4.82±0.72
Commercial drug	13.96±0.28 ^a	13.13±0.67 ^a	16.03±0.23	17.36±0.36	4.28±0.27	3.05±0.20 ^a	3.8±0.39 ^a	4.71±0.39

Mean values are expressed in terms of ±SD.

a & b - indicates the significant variations in each homogenous subsets at p<0.05 level (5%) by Tukeys HSD test.

SUMMARY AND CONCLUSION

The purpose and aim of the study was to develop a new iron compound capable of resulting in higher bioavailability and increased absorption, since iron deficiency has evolved as one of the top ten uneradicated health concern throughout the world. Mainly, the development of the iron compound was focused to apply for the food fortification process, because these fortification strategies have immense potential to eradicate iron deficiency. As per the guidelines of European Food Safety Authority (EFSA), 2009, the unexplored absorption capacity and solubility of the ferrous phosphate compound as an iron source was taken into consideration.

Ferrous phosphate is a water insoluble compound, with high absorption capacity and has a good nutritive value. This particular research focused on the development of size reduced ferrous phosphate compounds with increased solubility and absorption. Considering the nanotechnological developments and advantages in the health care and biomedical sector, it is understood that a compound when reduced with size and increased surface area, can result in a better bioavailability. In these means, the objective of the work was designed with the aim of reducing the ferrous phosphate particle size with high surface area, thereby to produce better bioavailability.

Ferrous phosphate nanoparticles were synthesized by controlled hydrolysis method using ferrous sulphate and sodium phosphate as the reaction precursors. The molar concentration of the synthesis process was varied, in order understand the effect of molar ratio in the characteristics of the nanoparticle. The synthesised particles were characterized by XRF and FTIR spectroscopic analysis, to observe the elemental content of the particles. The morphological characteristics were studied using SEM and AFM, which shows the sponge like structure during aggregation and spherical shaped particles when disintegrated, respectively. The size distributions in range of 70 – 110 nm were observed using centrifugal particle size analyser (CPS). BET analysis and zeta potential analysis showed the maximum

surface area of $220\text{ m}^2/\text{g}$ and positive charge of $+6.2\text{ mV}$ respectively for the stoichiometric reaction synthesis. Low particle size and high surface area are the advantageous factor of the particles for the bioavailability analysis, obtained by stoichiometric concentration. Furthermore, the high *in vitro* solubility of these particles were observed at pH 5 relative to pH 2. The dissolute Fe ions in HCl solution were evaluated by using ferrozine indicator colour complex absorbance at 562 nm. These, experimental data reveals that the significant properties of size and surface chemistry, present with the particles are capable of producing substantial improvement in the bioavailability linked to the direct uptake of the nanoparticle.

Sensory changes and effects were found to be the major concern for the iron compounds during food fortification, which results in poor bioavailability. In order to overcome these issues, the ferrous phosphate nanoparticles were encapsulated with the biodegradable polymers, which can protect the iron compound from the absorption inhibitors like phytates, tannins etc. The wide utility polymers in drug delivery, Chitosan and PLGA were selected as the polymer source. The microspheres of chitosan and PLGA were obtained using solvent emulsion method. Preformulation studies were carried out to optimize the concentration and stirring speed, to obtain the ideal microspheres. Three levels of drug to polymer ratio and stirring speed were varied and totally 9 batches of chitosan and PLGA microspheres were prepared. The morphology of all the batches of chitosan and PLGA microspheres were smooth and spherical shaped except few.

A 3^2 general full factorial design using the Design Expert Software 8.0 with Response Surface Methodology technique was developed for both Chitosan and PLGA microspheres. The drug to polymer ratio (X_1) and stirring speed (X_2) were kept as the independent variables and the mean particle size, drug entrapment efficiency and enhanced drug release were kept as the dependent variables. The polynomial equations with the mathematical sign of intercepts were obtained for each response effect with good correlation coefficient. It was found that, for chitosan microspheres the optimal mean particle size was around $14\mu\text{m}$, drug

entrapment efficiency with 72% and the complete drug release profile at 325 min. The batch B3 was found to be an optimal one. The following maximum criterion was adopted for the optimum PLGA microspheres: mean particle size of 2 μm , drug entrapment efficiency with 85% and the drug release saturation level at 270 minutes. The batch B3 was found to be an optimal one. The *in vivo* analysis was done for observing the haematological parameters of rat model, administered with ferrous phosphate nanoparticle direct uptake, chitosan microspheres, PLGA microspheres and ferrous sulphate as the standard drug.

In the present investigation it was observed that, the ferrous phosphate nanoparticle direct uptake as an iron compound, found to produce an improved effect comparing to the standard. Furthermore, the encapsulation of the drug with chitosan and PLGA also tend to produce an improvement in bioavailability of the drug, even though the drugs were released slowly in the gastrointestinal tract. Thus our results, collectively demonstrate that the direct uptake of ferrous nanoparticle increases the bioavailability of iron in a superior way, producing a good increase in the haematological parameters. Finally on the basis of *in vitro* and *in vivo* studies, it can be concluded that the PLGA microspheres could be better alternate to the poorly available iron compounds, with an advantage of combating sensory effects, when compared to the chitosan microspheres. The use of ferrous phosphate nanoparticles direct uptake and PLGA microspheres can be potentially employed for iron deficiency anaemia, in future.